

Article

# Electron Impact Excitation of F-Like W LXVI

Kanti M. Aggarwal

Astrophysics Research Centre, School of Mathematics and Physics, Queen's University Belfast, Belfast BT7 1NN, Northern Ireland, UK; K.Aggarwal@qub.ac.uk

Academic Editor: James F. Babb

Received: 13 May 2016; Accepted: 20 July 2016; Published: 26 July 2016

**Abstract:** Electron impact excitation collision strengths are calculated for all transitions among 113 levels of the  $2s^22p^5$ ,  $2s2p^6$ ,  $2s^22p^43l$ ,  $2s2p^53l$ , and  $2p^63l$  configurations of F-like W LXVI. For this purpose, Dirac Atomic R-matrix Code (DARC) has been adopted and results are listed over a wide energy range of 1000 to 6000 Ryd. For comparison purposes, analogous calculations have also been performed with the Flexible Atomic Code (FAC), and the results obtained are comparable with those from DARC.

**Keywords:** F-like tungsten; relativistic R-matrix method; collision strengths

## 1. Introduction

Tungsten (W) is a very important constituent of fusion reactor walls because of its materialistic characteristics. Additionally, it radiates at almost all ionisation stages, and, therefore, atomic data (namely energy levels, radiative rates, and collision strengths) are required for many of its ions. These data are required for modelling and diagnosing fusion plasmas for the elemental density, temperature, and chemical composition determination. Realising this, there have been many experimental and theoretical efforts to obtain atomic data for W ions. Experimentally, only level energies have been determined for many of the W ions, as compiled and assessed by Kramida and Shirai [1], and updated by Kramida [2]. Their recommended energies are also available on the NIST (National Institute of Standards and Technology) website—see [1] and references therein. However, for most ions, the measured energies are available for only a few levels and there are no corresponding measurements for other parameters, i.e., radiative rates (A-values) and collision strengths ( $\Omega$ ). For this reason, it becomes necessary to calculate data for the desired atomic parameters.

Theoretically, energy levels and A-values have been determined by many workers [3–7] for several W ions. We too have calculated these parameters for a few W ions, such as W XL [8], W LVIII [9], and W LIX to W LXVI [10]. Here, we focus our attention on F-like W LXVI. Additionally, for the other W ions, we have only reported energy levels and A-values, but here we also calculate results for  $\Omega$ .

Earlier calculations have been performed by Sampson et al. [11] for F-like ions with  $22 \leq Z \leq 92$ , including W LXVI. They adopted a relativistic atomic structure code to calculate oscillator strengths (f-values) and the *distorted-wave* (DW) method for the determination of  $\Omega$ . However, they presented only limited results for transitions from the lowest three levels of  $2s^22p^5$  and  $2s2p^6$  to higher excited 110 levels of the  $2s^22p^43l$ ,  $2s2p^53l$ , and  $2p^63l$  configurations. Additionally, they reported values of  $\Omega$  at only six energies, approximately in the 140–4400 Ryd range, depending on the transition because their results are in terms of *excited* energies. Furthermore, the format adopted by them is not straightforward to understand and apply their data. Therefore, recently S. Aggarwal [12] (henceforth, to be referred to as SA) has reported results for energy levels, f-values, A-values, line strengths (S-values), and lifetimes ( $\tau$ ) for the lowest 60 levels of the  $2s^22p^5$ ,  $2s2p^6$ , and  $2s^22p^43l$  configurations of W LXVI. For his calculations, he adopted the modified version of the GRASP (general-purpose relativistic atomic structure package) code, known as GRASP0. It is a fully relativistic code, is based on

the *jj* coupling scheme, and includes two-body relativistic corrections arising from the Breit interaction and QED (quantum electrodynamics) effects.

Unfortunately, the calculations of SA (apart from being very limited in range) are found to be erroneous and unreliable, particularly for  $\tau$ , as recently discussed and demonstrated by us [13]. Nevertheless, his calculations were extended to all 113 levels of the  $2s^2 2p^5$ ,  $2s 2p^6$ ,  $2s^2 2p^4 3\ell$ ,  $2s 2p^5 3\ell$ , and  $2p^6 3\ell$  configurations by Goyal et al. [14], who also calculated  $\Omega$  but at only four energies in the 1000–1600 Ryd range for the resonant *forbidden* transitions alone. This is because they included only a limited range of partial waves with angular momentum  $J \leq 9$ , *insufficient* for the convergence of  $\Omega$  for most allowed (and some forbidden) transitions. Therefore, in this work, we extend the range of partial waves to  $J \leq 50$  and energy to  $\leq 6400$  Ryd, so that  $\Omega$  can be determined for *all* transitions and over a wide energy range.

As by Goyal et al. [14], we adopt the *Dirac atomic R-matrix code* (DARC) and include the same 113 levels of the  $2s^2 2p^5$ ,  $2s 2p^6$ ,  $2s^2 2p^4 3\ell$ ,  $2s 2p^5 3\ell$ , and  $2p^6 3\ell$  configurations. Since results for energy levels and A-values (for four types of transitions, namely electric dipole (E1), electric quadrupole (E2), magnetic dipole (M1), and magnetic quadrupole (M2)) have already been reported by us [10], we focus here only on the  $\Omega$  data.

## 2. Calculations

The 113 levels of the  $2s^2 2p^5$ ,  $2s 2p^6$ ,  $2s^2 2p^4 3\ell$ ,  $2s 2p^5 3\ell$ , and  $2p^6 3\ell$  configurations are listed in Table 1 along with our calculated energies with the GRASP code. These energies are comparable to those listed by Goyal et al. [14], and their accuracy has already been discussed in our earlier work [13]. However, we note that the energies obtained by Goyal et al., with the corresponding FAC code and listed in their Table 1, are *incorrect*, particularly for the highest 20 levels. These energies are in clear error, by up to  $\sim 60$  Ryd. For this reason, in Table 1, we have also listed the ‘correct’ energies obtained with the FAC code. There is a satisfactory agreement between the GRASP and FAC energies, and the discrepancies are below 0.6 Ryd. Similarly, the orderings are nearly the same between the two calculations, although there are a few minor differences (see, for example, levels 10–12, 17–18, and 43–44).

For consistency, we employ the same DARC code for the calculations of  $\Omega$ , as by Goyal et al. [14]. It is based on the *jj* coupling scheme, and uses the Dirac–Coulomb Hamiltonian in the *R*-matrix approach. The *R*-matrix radius adopted for W LXVI is 0.66 au, and 25 continuum orbitals have been included for each channel angular momentum in the expansion of the wavefunction, allowing us to compute  $\Omega$  up to an energy of 6400 Ryd, i.e.,  $\sim 5500$  Ryd *above* the highest threshold. This energy range is sufficient to calculate values of effective collision strength ( $Y$ ) up to  $T_e = 3 \times 10^8$  K, well above what may be required for application to fusion plasmas where high temperatures prevail. The maximum number of channels for a partial wave is 512, and the corresponding size of the Hamiltonian matrix is 12,816. To obtain convergence of  $\Omega$  for all transitions and at all energies, we have included all partial waves with angular momentum  $J \leq 50$ . Furthermore, to account for higher neglected partial waves, we have included a top-up, based on the Coulomb–Bethe approximation [15] for allowed transitions and geometric series for others.

Table 1 also lists our calculated  $\Omega$  for all resonance transitions at an energy of 1600 Ryd, the highest energy considered by Goyal et al. [14]. For a ready comparison, their corresponding results are also listed at this energy. Their results are restricted to only a few (not all) *forbidden* transitions, as they did not calculate  $\Omega$  for the allowed ones, because the partial waves range was restricted to  $J \leq 9$ . As a result of this, for a few transitions, such as 1–8 ( $2s^2 2p^2 \ ^2P_{3/2}^o - 2s^2 2p^4 3p \ ^2D_{5/2}^o$ ), 1–12 ( $2s^2 2p^2 \ ^2P_{3/2}^o - 2s^2 2p^4 3p \ ^4D_{7/2}^o$ ), 1–41 ( $2s^2 2p^2 \ ^2P_{3/2}^o - 2s^2 2p^4 3p \ ^2F_{7/2}^o$ ), 1–73 ( $2s^2 2p^2 \ ^2P_{3/2}^o - 2s 2p^5 3d \ ^4F_{7/2}^o$ ), and 1–79 ( $2s^2 2p^2 \ ^2P_{3/2}^o - 2s 2p^5 3d \ ^4D_{7/2}^o$ ), their values of  $\Omega$  are *underestimated*, by up to 25%. The reason for this is clearly apparent from Figure 1a–c, in which we show the variation of  $\Omega$  with  $J$ , at six energies of 1000, 2000, 3000, 4000, 5000, and 6000 Ryd, and for three transitions, namely 1–3 ( $2s^2 2p^2 \ ^2P_{3/2}^o - 2s 2p^6 \ ^2S_{1/2}$ ), 1–8 ( $2s^2 2p^2 \ ^2P_{3/2}^o - 2s^2 2p^4 3p \ ^2D_{5/2}^o$ ), and 2–3 ( $2s^2 2p^2 \ ^2P_{1/2}^o - 2s 2p^6 \ ^2S_{1/2}$ ). The

1–3 and 2–3 transitions are allowed, and, therefore, they converge slowly with  $J$ . In fact, a slightly longer range of  $J$  would have been preferable to have fully converged  $\Omega$  for such transitions. However, due to computational limitations, it is not possible, and, therefore, a ‘top-up’ has been included for the additional contributing partial waves, based on the Coulomb–Bethe approximation of Burgess and Sheorey [15], as already stated. On the other hand, the 1–8 (see Figure 1b) is a forbidden transition but  $J \leq 9$  are not sufficient for the convergence of  $\Omega$ , even at an energy of 1000 Ryd. Therefore, the reported  $\Omega$  of Goyal et al. [14] are clearly underestimated, apart from being limited in the energy range as well as the (number of) transitions.

**Table 1.** Comparison of GRASP and FAC energies (in Ryd) for the levels of W LXVI, and collision strengths ( $\Omega$ ) for the resonance transitions at an energy of 1600 Ryd.  $a \pm b \equiv a \times 10^{\pm b}$ .

Index	Configuration	Level	GRASP	FAC	$\Omega_1$	$\Omega_2$
1	2s <sup>2</sup> 2p <sup>5</sup>	2P <sub>3/2</sub> <sup>o</sup>	0.0000	0.0000		
2	2s <sup>2</sup> 2p <sup>5</sup>	2P <sub>1/2</sub> <sup>o</sup>	102.0364	102.1521	2.028–3	1.860–3
3	2s2p <sup>6</sup>	2S <sub>1/2</sub>	137.7025	137.4448	3.990–2	
4	2s <sup>2</sup> 2p <sup>4</sup> 3s	4P <sub>5/2</sub>	621.0158	621.0472	4.571–4	
5	2s <sup>2</sup> 2p <sup>4</sup> 3s	2P <sub>3/2</sub>	621.8299	621.8704	1.258–3	
6	2s <sup>2</sup> 2p <sup>4</sup> 3s	2S <sub>1/2</sub>	625.8014	625.8038	3.349–4	
7	2s <sup>2</sup> 2p <sup>4</sup> ( <sup>3</sup> P)3p	4P <sub>3/2</sub> <sup>o</sup>	631.1841	631.1019	3.460–4	3.010–4
8	2s <sup>2</sup> 2p <sup>4</sup> ( <sup>3</sup> P)3p	2D <sub>5/2</sub> <sup>o</sup>	631.3275	631.2490	9.917–4	7.550–4
9	2s <sup>2</sup> 2p <sup>4</sup> ( <sup>1</sup> S)3p	2P <sub>1/2</sub> <sup>o</sup>	635.7137	635.6013	2.716–4	2.160–4
10	2s <sup>2</sup> 2p <sup>4</sup> ( <sup>3</sup> P)3p	4P <sub>5/2</sub> <sup>o</sup>	659.8186	659.7615	4.288–4	3.770–4
11	2s <sup>2</sup> 2p <sup>4</sup> ( <sup>3</sup> P)3p	2S <sub>1/2</sub> <sup>o</sup>	659.8909	659.8336	1.490–4	1.350–4
12	2s <sup>2</sup> 2p <sup>4</sup> ( <sup>3</sup> P)3p	4D <sub>7/2</sub> <sup>o</sup>	659.8176	659.7604	4.919–4	4.080–4
13	2s <sup>2</sup> 2p <sup>4</sup> ( <sup>3</sup> P)3p	4S <sub>3/2</sub> <sup>o</sup>	663.4845	663.4209	4.894–3	4.810–3
14	2s <sup>2</sup> 2p <sup>4</sup> ( <sup>1</sup> S)3p	2P <sub>3/2</sub> <sup>o</sup>	665.3718	665.2889	8.125–3	8.160–3
15	2s <sup>2</sup> 2p <sup>4</sup> ( <sup>3</sup> P)3d	4D <sub>3/2</sub>	670.6545	670.5186	5.541–4	
16	2s <sup>2</sup> 2p <sup>4</sup> ( <sup>3</sup> P)3d	4D <sub>5/2</sub>	670.8287	670.6959	1.302–3	
17	2s <sup>2</sup> 2p <sup>4</sup> ( <sup>3</sup> P)3d	4P <sub>1/2</sub>	671.0968	670.9598	1.531–3	
18	2s <sup>2</sup> 2p <sup>4</sup> ( <sup>3</sup> P)3d	2F <sub>7/2</sub>	670.8850	670.7513	7.566–4	
19	2s <sup>2</sup> 2p <sup>4</sup> ( <sup>1</sup> S)3d	2D <sub>3/2</sub>	675.3438	675.1778	4.138–4	
20	2s <sup>2</sup> 2p <sup>4</sup> ( <sup>3</sup> P)3d	4D <sub>7/2</sub>	677.3153	677.2001	4.780–4	
21	2s <sup>2</sup> 2p <sup>4</sup> ( <sup>3</sup> P)3d	4F <sub>9/2</sub>	677.3630	677.2476	5.318–4	
22	2s <sup>2</sup> 2p <sup>4</sup> ( <sup>3</sup> P)3d	2P <sub>1/2</sub>	678.4084	678.2780	3.296–3	
23	2s <sup>2</sup> 2p <sup>4</sup> ( <sup>3</sup> P)3d	2D <sub>5/2</sub>	680.2199	680.0693	1.682–2	
24	2s <sup>2</sup> 2p <sup>4</sup> ( <sup>1</sup> D)3d	2P <sub>3/2</sub>	680.3181	680.1636	1.607–2	
25	2s <sup>2</sup> 2p <sup>4</sup> ( <sup>1</sup> S)3d	2D <sub>5/2</sub>	682.9101	682.7466	1.599–2	
26	2s <sup>2</sup> 2p <sup>4</sup> 3s	4P <sub>3/2</sub>	723.5924	723.7012	1.089–4	
27	2s <sup>2</sup> 2p <sup>4</sup> 3s	2P <sub>1/2</sub>	724.3128	724.4307	8.681–5	
28	2s <sup>2</sup> 2p <sup>4</sup> 3s	2D <sub>5/2</sub>	725.0859	725.1903	2.380–4	
29	2s <sup>2</sup> 2p <sup>4</sup> 3s	2D <sub>3/2</sub>	725.5494	725.6597	1.058–4	
30	2s <sup>2</sup> 2p <sup>4</sup> ( <sup>3</sup> P)3p	4P <sub>1/2</sub> <sup>o</sup>	733.3901	733.3812	5.235–5	5.250–5
31	2s <sup>2</sup> 2p <sup>4</sup> ( <sup>3</sup> P)3p	4D <sub>3/2</sub> <sup>o</sup>	733.8677	733.8586	4.172–4	4.190–4
32	2s <sup>2</sup> 2p <sup>4</sup> ( <sup>1</sup> D)3p	2F <sub>5/2</sub> <sup>o</sup>	734.9009	734.8889	1.591–4	1.600–4
33	2s <sup>2</sup> 2p <sup>4</sup> ( <sup>1</sup> D)3p	2P <sub>3/2</sub> <sup>o</sup>	738.0872	738.0779	7.557–3	7.590–3
34	2s2p <sup>5</sup> ( <sup>3</sup> P)3s	4P <sub>5/2</sub> <sup>o</sup>	753.9775	753.7860	1.476–4	1.490–4
35	2s2p <sup>5</sup> ( <sup>3</sup> P)3s	2P <sub>3/2</sub> <sup>o</sup>	756.0908	755.8926	3.669–3	3.680–3
36	2s2p <sup>5</sup> ( <sup>1</sup> P)3s	2P <sub>1/2</sub> <sup>o</sup>	760.3451	760.2761	6.399–5	6.400–5
37	2s2p <sup>5</sup> ( <sup>1</sup> P)3s	2P <sub>3/2</sub> <sup>o</sup>	761.3225	761.1850	5.118–3	5.140–3
38	2s <sup>2</sup> 2p <sup>4</sup> ( <sup>3</sup> P)3p	4D <sub>5/2</sub> <sup>o</sup>	762.4810	762.4912	1.912–4	1.780–4
39	2s <sup>2</sup> 2p <sup>4</sup> ( <sup>3</sup> P)3p	2D <sub>3/2</sub> <sup>o</sup>	762.8417	762.8679	2.548–4	2.310–4
40	2s <sup>2</sup> 2p <sup>4</sup> ( <sup>3</sup> P)3p	2P <sub>1/2</sub> <sup>o</sup>	763.3247	763.2028	5.819–5	5.130–5

Table 1. Cont.

Index	Configuration	Level	GRASP	FAC	$\Omega 1$	$\Omega 2$
41	$2s^2 2p^4(^1D)3p$	$^2F_{7/2}^o$	763.6274	763.6406	3.567−4	2.770−4
42	$2s2p^5(^3P)3p$	$^4P_{3/2}$	764.6947	764.3845	6.249−4	
43	$2s^2 2p^4(^1D)3p$	$^2D_{3/2}^o$	764.5814	764.4924	2.231−4	2.230−4
44	$2s2p^5(^3P)3p$	$^2D_{5/2}$	764.7548	764.4542	2.448−3	
45	$2s^2 2p^4(^1D)3p$	$^2D_{5/2}^o$	764.5917	764.6064	2.274−4	2.020−4
46	$2s^2 2p^4(^1D)3p$	$^2P_{1/2}^o$	768.7542	768.7653	6.868−5	6.310−5
47	$2s2p^5(^1P)3p$	$^2P_{1/2}$	770.7609	770.4710	1.053−3	
48	$2s2p^5(^1P)3p$	$^2D_{3/2}$	770.9584	770.6495	1.305−3	
49	$2s^2 2p^4(^3P)3d$	$^4D_{1/2}$	772.6818	772.6419	4.247−5	
50	$2s^2 2p^4(^3P)3d$	$^4F_{3/2}$	773.5498	773.5032	2.544−4	
51	$2s^2 2p^4(^3P)3d$	$^4F_{5/2}$	773.9835	773.9305	2.910−3	
52	$2s^2 2p^4(^1D)3d$	$^2G_{7/2}$	774.4988	774.4520	1.712−4	
53	$2s^2 2p^4(^1D)3d$	$^2S_{1/2}$	776.1136	775.9935	3.725−3	
54	$2s^2 2p^4(^1D)3d$	$^2F_{5/2}$	776.1806	776.1017	9.448−3	
55	$2s^2 2p^4(^1D)3d$	$^2D_{3/2}$	776.5900	776.4849	7.625−3	
56	$2s^2 2p^4(^3P)3d$	$^4F_{7/2}$	779.7429	779.7072	2.751−4	
57	$2s^2 2p^4(^3P)3d$	$^2F_{5/2}$	780.7621	780.7166	2.195−4	
58	$2s^2 2p^4(^3P)3d$	$^2P_{3/2}$	780.8245	780.7799	1.418−4	
59	$2s^2 2p^4(^1D)3d$	$^2G_{9/2}$	781.2456	781.2032	3.748−4	
60	$2s^2 2p^4(^1D)3d$	$^2D_{5/2}$	781.9062	781.8558	2.032−4	
61	$2s^2 2p^4(^1D)3d$	$^2F_{7/2}$	782.3934	782.3387	2.880−4	
62	$2s^2 2p^4(^3P)3d$	$^2D_{3/2}$	784.1105	784.0251	2.330−4	
63	$2s^2 2p^4(^1D)3d$	$^2P_{1/2}$	784.5638	784.4725	1.470−4	
64	$2s2p^5(^3P)3p$	$^4D_{7/2}$	793.0956	792.8049	1.031−4	
65	$2s2p^5(^3P)3p$	$^2P_{3/2}$	793.6704	793.3832	5.946−4	
66	$2s2p^5(^3P)3p$	$^4P_{5/2}$	794.1495	793.8652	5.824−4	
67	$2s2p^5(^3P)3p$	$^2P_{1/2}$	795.7677	795.4634	3.999−4	
68	$2s2p^5(^1P)3p$	$^2D_{5/2}$	799.7264	799.4123	6.864−4	
69	$2s2p^5(^1P)3p$	$^2P_{3/2}$	800.2321	799.9214	2.773−4	
70	$2s2p^5(^1P)3p$	$^2S_{1/2}$	802.5375	802.2087	3.635−5	
71	$2s2p^5(^3P)3d$	$^4P_{1/2}^o$	803.4369	803.0729	6.151−5	5.990−5
72	$2s2p^5(^3P)3d$	$^4P_{3/2}^o$	804.1412	803.7745	1.978−4	1.850−4
73	$2s2p^5(^3P)3d$	$^4F_{7/2}^o$	804.3569	803.9899	1.530−3	1.260−3
74	$2s2p^5(^3P)3d$	$^4D_{5/2}^o$	804.6674	804.2952	5.927−4	5.360−4
75	$2s2p^5(^1P)3d$	$^2P_{1/2}^o$	810.4496	810.0549	5.359−4	4.760−4
76	$2s2p^5(^1P)3d$	$^2F_{5/2}^o$	810.3552	809.9675	2.897−4	2.720−4
77	$2s2p^5(^1P)3d$	$^2D_{3/2}^o$	810.6443	810.2531	2.168−4	2.020−4
78	$2s2p^5(^3P)3d$	$^4F_{9/2}^o$	810.1949	809.8459	2.236−4	
79	$2s2p^5(^3P)3d$	$^4D_{7/2}^o$	811.7383	811.3732	1.245−3	1.040−3
80	$2s2p^5(^3P)3d$	$^2D_{5/2}^o$	811.8379	811.4678	1.655−3	1.470−3
81	$2s2p^5(^3P)3d$	$^2D_{3/2}^o$	813.2720	812.8860	1.900−3	1.680−3
82	$2s2p^5(^3P)3d$	$^2P_{1/2}^o$	814.7593	814.3551	5.642−4	5.030−4
83	$2s2p^5(^1P)3d$	$^2F_{7/2}^o$	817.3939	817.0095	1.873−3	1.550−3
84	$2s2p^5(^1P)3d$	$^2D_{5/2}^o$	817.9735	817.5822	1.074−3	9.620−4
85	$2s2p^5(^1P)3d$	$^2P_{3/2}^o$	819.0236	818.6127	9.563−5	9.490−5
86	$2s^2 2p^4 3s$	$^4P_{1/2}$	829.6781	829.8751	7.003−8	
87	$2s^2 2p^4(^3P)3p$	$^4D_{1/2}^o$	840.7645	840.8461	2.038−7	2.050−7
88	$2s2p^5(^3P)3s$	$^4P_{1/2}^o$	858.3164	858.1844	1.087−7	1.030−7
89	$2s2p^5(^3P)3s$	$^4P_{3/2}^o$	860.6474	860.5151	1.450−6	1.450−6
90	$2s2p^5(^3P)3s$	$^2P_{1/2}^o$	862.8778	862.7383	3.711−7	3.590−7
91	$2s2p^5(^3P)3p$	$^4D_{1/2}$	868.2890	868.0427	8.322−8	
92	$2s^2 2p^4(^3P)3p$	$^2P_{3/2}^o$	868.5910	868.6870	4.743−8	4.660−8
93	$2s2p^5(^3P)3p$	$^4D_{3/2}$	870.6954	870.4452	1.956−7	
94	$2s2p^5(^3P)3p$	$^4P_{1/2}$	874.1049	873.8437	9.504−7	
95	$2s^2 2p^4(^3P)3d$	$^2D_{3/2}$	880.3596	880.3873	2.208−7	
96	$2s^2 2p^4(^3P)3d$	$^2D_{5/2}$	886.2175	886.2606	2.808−7	

Table 1. Cont.

Index	Configuration	Level	GRASP	FAC	$\Omega 1$	$\Omega 2$
97	2p <sup>6</sup> 3s	<sup>2</sup> S <sub>1/2</sub>	896.7062	896.4069	3.770–7	
98	2s2p <sup>5</sup> ( <sup>3</sup> P)3p	<sup>4</sup> P <sub>3/2</sub>	896.9621	896.7433	7.283–8	
99	2s2p <sup>5</sup> ( <sup>3</sup> P)3p	<sup>2</sup> D <sub>5/2</sub>	899.7352	899.5043	6.901–7	
100	2s2p <sup>5</sup> ( <sup>3</sup> P)3p	<sup>2</sup> D <sub>3/2</sub>	899.9941	899.7643	1.825–7	
101	2s2p <sup>5</sup> ( <sup>3</sup> P)3p	<sup>2</sup> S <sub>1/2</sub>	901.5742	901.1860	1.360–7	
102	2p <sup>6</sup> 3p	<sup>2</sup> P <sub>1/2</sub> <sup>o</sup>	907.0799	906.6040	3.935–7	3.290–7
103	2s2p <sup>5</sup> ( <sup>3</sup> P)3d	<sup>4</sup> F <sub>3/2</sub> <sup>o</sup>	907.9881	907.6989	2.621–7	2.390–7
104	2s2p <sup>5</sup> ( <sup>3</sup> P)3d	<sup>4</sup> F <sub>5/2</sub> <sup>o</sup>	910.6146	910.3175	9.255–7	8.750–7
105	2s2p <sup>5</sup> ( <sup>3</sup> P)3d	<sup>2</sup> D <sub>3/2</sub> <sup>o</sup>	911.8530	911.5314	1.587–6	1.440–6
106	2s2p <sup>5</sup> ( <sup>3</sup> P)3d	<sup>4</sup> D <sub>1/2</sub> <sup>o</sup>	912.6107	912.2002	9.235–7	8.030–7
107	2s2p <sup>5</sup> ( <sup>3</sup> P)3d	<sup>4</sup> P <sub>5/2</sub> <sup>o</sup>	914.6738	914.3862	1.013–7	9.570–8
108	2s2p <sup>5</sup> ( <sup>3</sup> P)3d	<sup>2</sup> F <sub>7/2</sub> <sup>o</sup>	917.2549	916.9567	1.914–6	1.700–6
109	2s2p <sup>5</sup> ( <sup>3</sup> P)3d	<sup>2</sup> F <sub>5/2</sub> <sup>o</sup>	917.9829	917.6765	1.169–6	1.110–6
110	2s2p <sup>5</sup> ( <sup>3</sup> P)3d	<sup>2</sup> P <sub>3/2</sub> <sup>o</sup>	918.1001	917.7930	2.255–7	2.190–7
111	2p <sup>6</sup> 3p	<sup>2</sup> P <sub>3/2</sub> <sup>o</sup>	936.4360	935.8958	2.730–7	2.640–7
112	2p <sup>6</sup> 3d	<sup>2</sup> D <sub>3/2</sub>	947.1796	946.5540	4.332–7	
113	2p <sup>6</sup> 3d	<sup>2</sup> D <sub>5/2</sub>	954.0121	953.3910	1.309–6	

GRASP: Present energies with the GRASP code from 11 configurations and 113 levels

FAC: Present energies with the FAC code from 11 configurations and 113 levels

$\Omega 1$ : Present results from the DARC code

$\Omega 2$ : Earlier results of Goyal et al. [14] from the DARC code

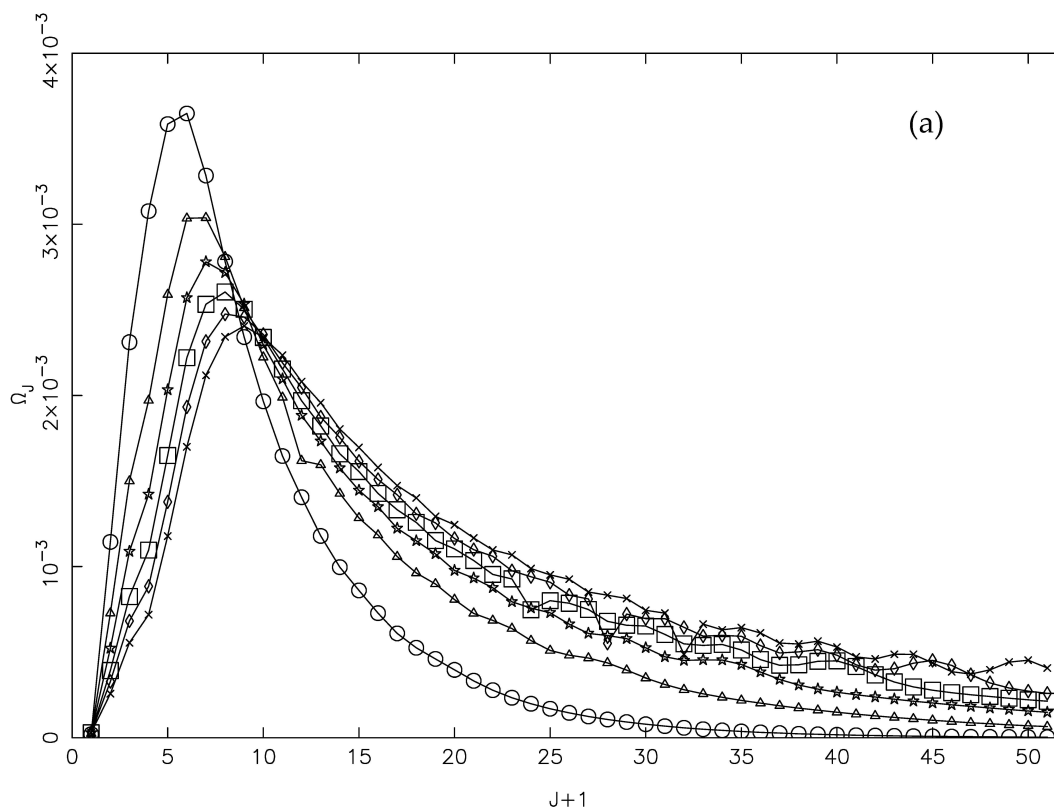
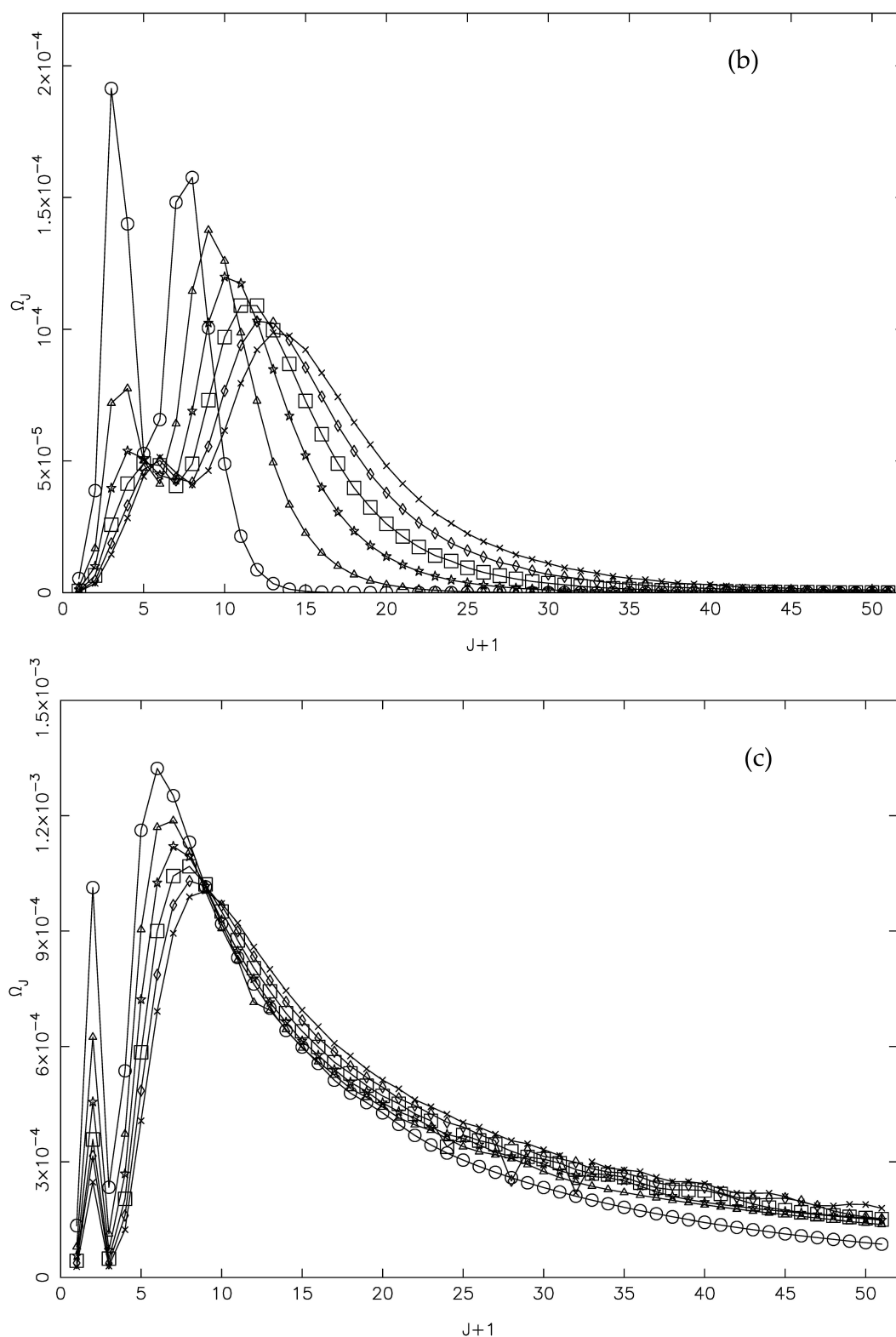


Figure 1. Cont.



**Figure 1.** Partial collision strengths for the (a) 1–3 ( $2s^22p^5 \ ^2P_{3/2}^o - 2s2p^6 \ ^2S_{1/2}$ ), (b) 1–8 ( $2s^22p^5 \ ^2P_{3/2}^o - 2s2p^6 \ ^4P_{5/2}^o$ ), and (c) 2–3 ( $2s^22p^5 \ ^2P_{1/2}^o - 2s2p^6 \ ^2S_{1/2}$ ) transitions of W LXVI, at six energies of: 1000 Ryd (circles), 2000 Ryd (triangles), 3000 Ryd (stars), 4000 Ryd (squares), 5000 Ryd (diamonds), and 6000 Ryd (crosses).

In Table 2, we list our calculated  $\Omega$  at 10 energies (1000, 1200, 1400, 1600, 1800, 2000, 3000, 4000, 5000, and 6000 Ryd) for all transitions from the lowest three to the higher excited levels. The corresponding results for all other remaining transitions may be obtained on request from the author. For the same transitions as listed in Table 2, Sampson et al. [11] have also reported  $\Omega$ , but only in a limited energy range, as already stated. In Figure 2, we compare our results with them, in the common energy range (below 4000 Ryd) for the same three transitions (1–3, 1–8, and 2–3), as shown in Figure 1. The agreement between the two calculations is fully satisfactory, and there is no (significant) discrepancy for these three (and other) transitions of W LXVI.

**Table 2.** Collision strengths ( $\Omega$ ) for transitions from the lowest three to higher excited levels of W LXVI in the energy range 1000 to 6000 Ryd.  $a \pm b \equiv a \times 10^{\pm b}$ .

I	J	1000	1200	1400	1600	1800	2000	3000	4000	5000	6000
1	2	2.230–3	2.146–3	2.068–3	2.028–3	1.987–3	1.971–3	1.949–3	1.997–3	2.079–3	2.186–3
1	3	3.521–2	3.696–2	3.853–2	3.990–2	4.117–2	4.263–2	4.861–2	5.359–2	5.835–2	6.775–2
1	4	4.442–4	4.412–4	4.447–4	4.571–4	4.730–4	4.935–4	6.082–4	7.325–4	8.553–4	9.717–4
1	5	7.918–4	9.518–4	1.108–3	1.258–3	1.407–3	1.553–3	2.199–3	2.777–3	3.308–3	3.798–3
1	6	2.417–4	2.722–4	3.033–4	3.349–4	3.671–4	3.998–4	5.490–4	6.869–4	8.149–4	9.341–4
1	7	4.646–4	4.141–4	3.730–4	3.460–4	3.256–4	3.112–4	2.802–4	2.777–4	2.848–4	2.975–4
1	8	9.847–4	9.790–4	9.791–4	9.917–4	1.008–3	1.024–3	1.129–3	1.234–3	1.334–3	1.434–3
1	9	2.934–4	2.824–4	2.744–4	2.716–4	2.709–4	2.716–4	2.872–4	3.083–4	3.304–4	3.531–4
1	10	6.135–4	5.339–4	4.704–4	4.288–4	3.979–4	3.751–4	3.250–4	3.174–4	3.241–4	3.376–4
1	11	2.225–4	1.912–4	1.662–4	1.490–4	1.364–4	1.267–4	1.034–4	9.706–5	9.664–5	9.912–5
1	12	7.045–4	6.117–4	5.383–4	4.919–4	4.567–4	4.315–4	3.787–4	3.738–4	3.850–4	4.029–4
1	13	4.496–3	4.674–3	4.772–3	4.894–3	4.991–3	5.090–3	5.505–3	5.839–3	6.170–3	6.520–3
1	14	7.576–3	7.836–3	7.956–3	8.125–3	8.254–3	8.392–3	8.967–3	9.437–3	9.921–3	1.045–2
1	15	8.063–4	6.866–4	6.097–4	5.541–4	5.199–4	4.947–4	4.596–4	4.778–4	5.131–4	5.536–4
1	16	1.414–3	1.341–3	1.311–3	1.302–3	1.314–3	1.335–3	1.508–3	1.710–3	1.915–3	2.114–3
1	17	1.319–3	1.382–3	1.456–3	1.531–3	1.612–3	1.695–3	2.092–3	2.459–3	2.808–3	3.137–3
1	18	9.140–4	8.326–4	7.850–4	7.566–4	7.444–4	7.368–4	7.612–4	8.103–4	8.658–4	9.207–4
1	19	5.670–4	4.928–4	4.460–4	4.138–4	3.950–4	3.812–4	3.680–4	3.843–4	4.096–4	4.372–4
1	20	9.046–4	7.088–4	5.749–4	4.780–4	4.103–4	3.574–4	2.300–4	1.866–4	1.705–4	1.654–4
1	21	8.985–4	7.274–4	6.116–4	5.318–4	4.776–4	4.367–4	3.504–4	3.322–4	3.352–4	3.458–4
1	22	2.573–3	2.824–3	3.068–3	3.296–3	3.523–3	3.748–3	4.753–3	5.642–3	6.470–3	7.247–3
1	23	1.246–2	1.404–2	1.550–2	1.682–2	1.811–2	1.938–2	2.490–2	2.966–2	3.407–2	3.816–2
1	24	1.192–2	1.342–2	1.481–2	1.607–2	1.730–2	1.851–2	2.377–2	2.832–2	3.254–2	3.647–2
1	25	1.199–2	1.343–2	1.477–2	1.599–2	1.718–2	1.837–2	2.356–2	2.807–2	3.225–2	3.614–2
1	26	1.182–4	1.122–4	1.090–4	1.089–4	1.100–4	1.131–4	1.353–4	1.619–4	1.895–4	2.156–4
1	27	7.096–5	7.500–5	8.047–5	8.681–5	9.372–5	1.016–4	1.402–4	1.773–4	2.126–4	2.454–4
1	28	2.066–4	2.132–4	2.243–4	2.380–4	2.534–4	2.722–4	3.662–4	4.579–4	5.461–4	6.276–4
1	29	1.174–4	1.105–4	1.066–4	1.058–4	1.062–4	1.087–4	1.283–4	1.527–4	1.783–4	2.027–4
1	30	9.405–5	7.654–5	6.154–5	5.235–5	4.343–5	3.778–5	1.981–5	1.207–5	8.068–6	5.954–6
1	31	4.712–4	4.489–4	4.249–4	4.172–4	4.036–4	4.007–4	3.892–4	3.935–4	4.060–4	4.218–4
1	32	2.859–4	2.326–4	1.871–4	1.591–4	1.320–4	1.149–4	6.021–5	3.668–5	2.451–5	1.806–5
1	33	6.915–3	7.194–3	7.315–3	7.557–3	7.642–3	7.838–3	8.394–3	8.856–3	9.340–3	9.814–3
1	34	2.707–4	2.171–4	1.750–4	1.476–4	1.242–4	1.074–4	5.827–5	3.698–5	2.639–5	1.900–5
1	35	3.321–3	3.462–3	3.543–3	3.669–3	3.724–3	3.826–3	4.135–3	4.390–3	4.645–3	4.888–3
1	36	1.144–4	9.253–5	7.521–5	6.399–5	5.417–5	4.734–5	2.702–5	1.838–5	1.414–5	1.141–5
1	37	4.602–3	4.812–3	4.935–3	5.118–3	5.200–3	5.349–3	5.793–3	6.157–3	6.517–3	6.861–3
1	38	2.808–4	2.411–4	2.096–4	1.912–4	1.733–4	1.635–4	1.357–4	1.302–4	1.319–4	1.370–4
1	39	2.689–4	2.604–4	2.540–4	2.548–4	2.535–4	2.570–4	2.746–4	2.966–4	3.194–4	3.416–4
1	40	7.328–5	6.611–5	6.073–5	5.819–5	5.560–5	5.480–5	5.413–5	5.715–5	6.112–5	6.540–5
1	41	4.018–4	3.775–4	3.607–4	3.567–4	3.518–4	3.544–4	3.782–4	4.133–4	4.499–4	4.857–4
1	42	4.529–4	5.103–4	5.679–4	6.249–4	6.808–4	7.409–4	1.011–3	1.253–3	1.480–3	1.692–3
1	43	2.735–4	2.514–4	2.323–4	2.231–4	2.116–4	2.073–4	1.922–4	1.910–4	1.952–4	2.018–4
1	44	1.584–3	1.887–3	2.178–3	2.448–3	2.709–3	2.986–3	4.187–3	5.237–3	6.209–3	7.108–3
1	45	2.947–4	2.635–4	2.396–4	2.274–4	2.153–4	2.105–4	2.022–4	2.105–4	2.236–4	2.383–4
1	46	9.707–5	8.431–5	7.433–5	6.868–5	6.315–5	6.038–5	5.301–5	5.269–5	5.452–5	5.730–5
1	47	6.832–4	8.125–4	9.362–4	1.053–3	1.165–3	1.279–3	1.781–3	2.219–3	2.625–3	3.001–3
1	48	8.806–4	1.028–3	1.170–3	1.305–3	1.435–3	1.570–3	2.167–3	2.690–3	3.176–3	3.627–3
1	49	8.850–5	6.725–5	5.267–5	4.247–5	3.474–5	2.904–5	1.443–5	9.080–6	6.727–6	5.568–6
1	50	3.003–4	2.745–4	2.606–4	2.544–4	2.521–4	2.539–4	2.814–4	3.192–4	3.596–4	3.989–4

Table 2. Cont.

I	J	1000	1200	1400	1600	1800	2000	3000	4000	5000	6000
1	51	2.237−3	2.469−3	2.693−3	2.910−3	3.115−3	3.333−3	4.288−3	5.123−3	5.908−3	6.633−3
1	52	3.611−4	2.736−4	2.134−4	1.712−4	1.392−4	1.154−4	5.385−5	3.050−5	1.959−5	1.368−5
1	53	2.704−3	3.070−3	3.406−3	3.725−3	4.021−3	4.315−3	5.598−3	6.700−3	7.729−3	8.678−3
1	54	6.845−3	7.780−3	8.642−3	9.448−3	1.020−2	1.098−2	1.430−2	1.716−2	1.983−2	2.228−2
1	55	5.511−3	6.271−3	6.969−3	7.625−3	8.239−3	8.855−3	1.153−2	1.382−2	1.595−2	1.792−2
1	56	5.147−4	4.030−4	3.280−4	2.751−4	2.360−4	2.064−4	1.338−4	1.092−4	1.003−4	9.747−5
1	57	2.992−4	2.590−4	2.346−4	2.195−4	2.094−4	2.034−4	1.976−4	2.056−4	2.175−4	2.303−4
1	58	2.489−4	1.985−4	1.651−4	1.418−4	1.248−4	1.120−4	8.213−5	7.341−5	7.156−5	7.227−5
1	59	4.392−4	4.020−4	3.831−4	3.748−4	3.710−4	3.719−4	3.948−4	4.259−4	4.583−4	4.895−4
1	60	3.800−4	2.974−4	2.421−4	2.032−4	1.744−4	1.527−4	9.961−5	8.185−5	7.564−5	7.388−5
1	61	3.867−4	3.363−4	3.062−4	2.880−4	2.758−4	2.690−4	2.643−4	2.765−4	2.933−4	3.110−4
1	62	2.713−4	2.488−4	2.376−4	2.330−4	2.317−4	2.337−4	2.583−4	2.901−4	3.234−4	3.555−4
1	63	1.962−4	1.712−4	1.561−4	1.470−4	1.415−4	1.387−4	1.432−4	1.582−4	1.765−4	1.949−4
1	64	1.819−4	1.487−4	1.220−4	1.031−4	8.640−5	7.514−5	3.968−5	2.427−5	1.630−5	1.167−5
1	65	3.342−4	4.212−4	5.099−4	5.946−4	6.793−4	7.674−4	1.167−3	1.522−3	1.853−3	2.160−3
1	66	3.581−4	4.313−4	5.079−4	5.824−4	6.564−4	7.385−4	1.108−3	1.441−3	1.753−3	2.042−3
1	67	2.121−4	2.753−4	3.390−4	3.999−4	4.603−4	5.218−4	8.006−4	1.048−3	1.277−3	1.489−3
1	68	4.029−4	4.966−4	5.936−4	6.864−4	7.790−4	8.798−4	1.333−3	1.738−3	2.116−3	2.466−3
1	69	1.871−4	2.151−4	2.459−4	2.773−4	3.093−4	3.442−4	5.073−4	6.570−4	7.980−4	9.295−4
1	70	5.156−5	4.472−5	3.958−5	3.635−5	3.368−5	3.239−5	3.047−5	3.275−5	3.644−5	4.053−5
1	71	1.015−4	8.352−5	7.063−5	6.151−5	5.464−5	4.959−5	3.681−5	3.289−5	3.189−5	3.195−5
1	72	2.512−4	2.253−4	2.085−4	1.978−4	1.908−4	1.869−4	1.846−4	1.938−4	2.060−4	2.184−4
1	73	1.240−3	1.340−3	1.439−3	1.530−3	1.617−3	1.700−3	2.043−3	2.317−3	2.556−3	2.764−3
1	74	5.688−4	5.698−4	5.793−4	5.927−4	6.087−4	6.267−4	7.142−4	7.952−4	8.695−4	9.361−4
1	75	4.093−4	4.551−4	4.978−4	5.359−4	5.714−4	6.047−4	7.380−4	8.418−4	9.307−4	1.008−3
1	76	3.703−4	3.313−4	3.060−4	2.897−4	2.792−4	2.731−4	2.690−4	2.821−4	2.998−4	3.176−4
1	77	2.625−4	2.395−4	2.254−4	2.168−4	2.119−4	2.097−4	2.141−4	2.282−4	2.445−4	2.602−4
1	78	4.402−4	3.427−4	2.742−4	2.236−4	1.860−4	1.567−4	7.841−5	4.685−5	3.114−5	2.182−5
1	79	1.044−3	1.110−3	1.179−3	1.245−3	1.310−3	1.372−3	1.637−3	1.854−3	2.044−3	2.210−3
1	80	1.251−3	1.397−3	1.534−3	1.655−3	1.768−3	1.873−3	2.294−3	2.621−3	2.900−3	3.142−3
1	81	1.348−3	1.555−3	1.740−3	1.900−3	2.048−3	2.183−3	2.711−3	3.111−3	3.449−3	3.741−3
1	82	4.228−4	4.743−4	5.221−4	5.642−4	6.037−4	6.402−4	7.859−4	8.984−4	9.941−4	1.077−3
1	83	1.447−3	1.599−3	1.743−3	1.873−3	1.995−3	2.109−3	2.571−3	2.934−3	3.244−3	3.514−3
1	84	8.712−4	9.404−4	1.010−3	1.074−3	1.136−3	1.194−3	1.439−3	1.635−3	1.805−3	1.954−3
1	85	1.806−4	1.423−4	1.154−4	9.563−5	8.097−5	6.961−5	3.972−5	2.814−5	2.274−5	1.977−5
1	86	9.949−8	8.545−8	7.645−8	7.003−8	6.525−8	6.211−8	5.602−8	5.696−8	6.063−8	6.464−8
1	87	3.629−7	2.906−7	2.383−7	2.038−7	1.735−7	1.559−7	1.026−7	8.385−8	7.659−8	7.223−8
1	88	1.406−7	1.256−7	1.151−7	1.087−7	1.034−7	1.011−7	9.682−8	9.990−8	1.051−7	1.108−7
1	89	1.390−6	1.409−6	1.424−6	1.450−6	1.459−6	1.493−6	1.589−6	1.682−6	1.775−6	1.862−6
1	90	4.935−7	4.355−7	3.948−7	3.711−7	3.495−7	3.413−7	3.199−7	3.243−7	3.368−7	3.504−7
1	91	1.082−7	9.652−8	8.820−8	8.322−8	7.888−8	7.701−8	7.437−8	7.836−8	8.520−8	9.191−8
1	92	8.382−8	6.702−8	5.515−8	4.743−8	4.136−8	3.750−8	2.754−8	2.473−8	2.422−8	2.456−8
1	93	2.389−7	2.157−7	2.018−7	1.956−7	1.923−7	1.935−7	2.164−7	2.501−7	2.871−7	3.233−7
1	94	1.156−6	1.067−6	9.924−7	9.504−7	9.019−7	8.830−7	8.175−7	8.159−7	8.548−7	8.865−7
1	95	3.860−7	3.094−7	2.583−7	2.208−7	1.922−7	1.721−7	1.159−7	9.358−8	8.279−8	7.627−8
1	96	2.967−7	2.800−7	2.771−7	2.808−7	2.881−7	2.995−7	3.665−7	4.358−7	5.039−7	5.683−7
1	97	3.647−7	3.661−7	3.683−7	3.770−7	3.824−7	3.940−7	4.484−7	5.079−7	5.731−7	6.327−7
1	98	9.524−8	8.435−8	7.729−8	7.283−8	6.983−8	6.842−8	6.835−8	7.316−8	7.978−8	8.647−8
1	99	4.754−7	5.391−7	6.117−7	6.901−7	7.696−7	8.536−7	1.260−6	1.636−6	1.990−6	2.325−6
1	100	2.156−7	1.983−7	1.875−7	1.825−7	1.813−7	1.827−7	2.086−7	2.446−7	2.834−7	3.217−7
1	101	1.440−7	1.393−7	1.362−7	1.360−7	1.357−7	1.381−7	1.543−7	1.763−7	2.013−7	2.254−7
1	102	3.868−7	3.904−7	3.930−7	3.935−7	3.944−7	3.959−7	3.932−7	3.884−7	3.848−7	3.824−7
1	103	3.022−7	2.793−7	2.684−7	2.621−7	2.603−7	2.603−7	2.694−7	2.814−7	2.931−7	3.042−7
1	104	9.708−7	9.336−7	9.224−7	9.255−7	9.388−7	9.572−7	1.076−6	1.194−6	1.303−6	1.404−6
1	105	1.601−6	1.583−6	1.582−6	1.587−6	1.595−6	1.611−6	1.687−6	1.763−6	1.842−6	1.914−6
1	106	9.558−7	9.421−7	9.330−7	9.235−7	9.158−7	9.115−7	8.907−7	8.824−7	8.857−7	8.915−7
1	107	1.440−7	1.214−7	1.087−7	1.013−7	9.726−8	9.519−8	9.566−8	1.013−7	1.079−7	1.145−7
1	108	1.624−6	1.712−6	1.814−6	1.914−6	2.018−6	2.115−6	2.556−6	2.912−6	3.217−6	3.487−6
1	109	1.128−6	1.123−6	1.141−6	1.169−6	1.205−6	1.243−6	1.443−6	1.622−6	1.781−6	1.924−6
1	110	3.628−7	2.995−7	2.557−7	2.255−7	2.039−7	1.892−7	1.554−7	1.487−7	1.500−7	1.543−7
1	111	3.559−7	3.200−7	2.912−7	2.730−7	2.578−7	2.499−7	2.279−7	2.246−7	2.268−7	2.317−7
1	112	5.862−7	5.102−7	4.658−7	4.332−7	4.145−7	4.013−7	3.788−7	3.841−7	3.999−7	4.190−7
1	113	1.248−6	1.243−6	1.272−6	1.309−6	1.358−6	1.412−6	1.682−6	1.940−6	2.191−6	2.430−6



Table 2. Cont.

I	J	1000	1200	1400	1600	1800	2000	3000	4000	5000	6000
2	3	2.281-2	2.396-2	2.505-2	2.605-2	2.700-2	2.798-2	3.260-2	3.703-2	4.162-2	5.064-2
2	4	3.589-8	2.891-8	2.379-8	1.998-8	1.704-8	1.471-8	8.195-9	5.409-9	3.995-9	3.101-9
2	5	5.392-8	5.613-8	5.958-8	6.330-8	6.770-8	7.141-8	9.076-8	1.088-7	1.254-7	1.409-7
2	6	8.630-8	9.099-8	9.650-8	1.027-7	1.095-7	1.152-7	1.458-7	1.759-7	2.043-7	2.316-7
2	7	7.631-8	6.880-8	6.360-8	6.037-8	5.811-8	5.651-8	5.465-8	5.616-8	5.869-8	6.199-8
2	8	8.735-8	8.277-8	8.030-8	7.915-8	7.897-8	7.885-8	8.324-8	8.921-8	9.536-8	1.020-7
2	9	1.976-7	1.892-7	1.832-7	1.790-7	1.771-7	1.745-7	1.746-7	1.782-7	1.853-7	1.926-7
2	10	8.682-8	7.715-8	7.085-8	6.714-8	6.487-8	6.325-8	6.287-8	6.621-8	7.042-8	7.527-8
2	11	5.110-7	5.207-7	5.267-7	5.343-7	5.426-7	5.482-7	5.828-7	6.120-7	6.442-7	6.748-7
2	12	6.056-8	4.724-8	3.763-8	3.073-8	2.561-8	2.151-8	1.094-8	6.570-9	4.448-9	3.239-9
2	13	3.562-7	3.207-7	2.940-7	2.797-7	2.687-7	2.615-7	2.524-7	2.585-7	2.700-7	2.830-7
2	14	5.616-7	4.710-7	4.026-7	3.586-7	3.250-7	2.993-7	2.377-7	2.160-7	2.096-7	2.082-7
2	15	1.095-6	1.178-6	1.263-6	1.342-6	1.424-6	1.497-6	1.839-6	2.149-6	2.437-6	2.709-6
2	16	1.422-7	1.145-7	9.533-8	8.143-8	7.190-8	6.428-8	4.668-8	4.128-8	3.979-8	3.968-8
2	17	3.561-7	3.739-7	3.937-7	4.134-7	4.354-7	4.546-7	5.524-7	6.442-7	7.310-7	8.133-7
2	18	7.339-8	5.865-8	4.920-8	4.310-8	3.912-8	3.629-8	3.106-8	3.068-8	3.157-8	3.286-8
2	19	6.462-7	6.846-7	7.284-7	7.720-7	8.192-7	8.617-7	1.067-6	1.255-6	1.430-6	1.594-6
2	20	1.351-7	1.105-7	9.420-8	8.298-8	7.560-8	7.002-8	5.921-8	5.799-8	5.951-8	6.195-8
2	21	8.789-8	6.438-8	4.878-8	3.793-8	3.050-8	2.482-8	1.147-8	6.743-9	4.597-9	3.443-9
2	22	2.038-7	1.775-7	1.602-7	1.476-7	1.399-7	1.330-7	1.202-7	1.185-7	1.209-7	1.246-7
2	23	2.929-7	2.453-7	2.118-7	1.885-7	1.721-7	1.587-7	1.256-7	1.121-7	1.060-7	1.031-7
2	24	4.742-7	4.331-7	4.106-7	3.969-7	3.928-7	3.895-7	4.077-7	4.402-7	4.768-7	5.132-7
2	25	3.662-7	2.952-7	2.453-7	2.096-7	1.844-7	1.636-7	1.108-7	8.777-8	7.581-8	6.844-8
2	26	1.136-4	9.450-5	8.068-5	7.073-5	6.296-5	5.755-5	4.403-5	4.149-5	4.275-5	4.514-5
2	27	2.240-4	2.818-4	3.381-4	3.915-4	4.439-4	4.957-4	7.224-4	9.220-4	1.103-3	1.271-3
2	28	1.635-4	1.316-4	1.078-4	9.008-5	7.572-5	6.502-5	3.371-5	2.051-5	1.394-5	9.769-6
2	29	4.394-4	5.527-4	6.628-4	7.666-4	8.696-4	9.717-4	1.416-3	1.808-3	2.165-3	2.493-3
2	30	1.103-4	8.829-5	7.096-5	5.976-5	4.976-5	4.277-5	2.249-5	1.370-5	9.209-6	6.757-6
2	31	2.950-4	2.752-4	2.619-4	2.568-4	2.525-4	2.512-4	2.596-4	2.768-4	2.958-4	3.156-4
2	32	5.248-4	5.227-4	5.271-4	5.397-4	5.510-4	5.634-4	6.316-4	6.970-4	7.571-4	8.152-4
2	33	2.804-4	2.535-4	2.341-4	2.243-4	2.156-4	2.108-4	2.063-4	2.146-4	2.264-4	2.400-4
2	34	9.685-6	7.990-6	6.773-6	6.001-6	5.353-6	4.913-6	3.811-6	3.512-6	3.482-6	3.551-6
2	35	6.352-6	6.300-6	6.347-6	6.511-6	6.668-6	6.847-6	7.805-6	8.712-6	9.534-6	1.031-5
2	36	4.286-5	3.904-5	3.595-5	3.437-5	3.264-5	3.176-5	2.928-5	2.888-5	2.947-5	3.017-5
2	37	2.252-5	2.172-5	2.140-5	2.163-5	2.187-5	2.229-5	2.491-5	2.765-5	3.024-5	3.269-5
2	38	2.738-4	2.190-4	1.795-4	1.536-4	1.320-4	1.169-4	7.651-5	6.218-5	5.683-5	5.487-5
2	39	2.358-4	2.066-4	1.853-4	1.739-4	1.636-4	1.580-4	1.479-4	1.515-4	1.590-4	1.680-4
2	40	4.431-4	4.347-4	4.266-4	4.277-4	4.239-4	4.260-4	4.353-4	4.509-4	4.723-4	4.908-4
2	41	3.682-4	2.870-4	2.282-4	1.887-4	1.555-4	1.320-4	6.612-5	3.918-5	2.609-5	1.834-5
2	42	1.383-6	1.320-6	1.306-6	1.318-6	1.353-6	1.403-6	1.701-6	2.022-6	2.338-6	2.636-6
2	43	2.234-4	1.990-4	1.818-4	1.731-4	1.654-4	1.617-4	1.580-4	1.652-4	1.753-4	1.864-4
2	44	3.357-6	3.066-6	2.905-6	2.838-6	2.804-6	2.805-6	2.966-6	3.201-6	3.441-6	3.672-6
2	45	3.336-4	3.270-4	3.269-4	3.338-4	3.402-4	3.486-4	3.955-4	4.415-4	4.838-4	5.238-4
2	46	7.338-3	7.623-3	7.808-3	8.063-3	8.186-3	8.376-3	8.993-3	9.511-3	1.007-2	1.052-2
2	47	9.839-6	8.898-6	8.340-6	8.029-6	7.894-6	7.852-6	8.391-6	9.346-6	1.040-5	1.144-5
2	48	4.375-6	3.650-6	3.222-6	2.986-6	2.873-6	2.845-6	3.177-6	3.771-6	4.411-6	5.034-6
2	49	4.089-4	3.579-4	3.257-4	3.057-4	2.941-4	2.875-4	2.930-4	3.214-4	3.561-4	3.916-4
2	50	6.272-4	5.790-4	5.544-4	5.436-4	5.440-4	5.501-4	6.185-4	7.063-4	7.976-4	8.852-4
2	51	3.479-4	2.986-4	2.680-4	2.501-4	2.382-4	2.312-4	2.253-4	2.358-4	2.501-4	2.649-4
2	52	5.215-4	4.841-4	4.652-4	4.593-4	4.574-4	4.605-4	4.939-4	5.352-4	5.763-4	6.152-4
2	53	3.566-4	3.079-4	2.766-4	2.568-4	2.446-4	2.371-4	2.354-4	2.553-4	2.813-4	3.084-4
2	54	3.372-4	2.800-4	2.433-4	2.205-4	2.048-4	1.946-4	1.778-4	1.812-4	1.898-4	1.998-4
2	55	3.794-4	3.141-4	2.716-4	2.438-4	2.259-4	2.139-4	1.988-4	2.106-4	2.301-4	2.513-4
2	56	4.385-4	3.283-4	2.545-4	2.038-4	1.668-4	1.395-4	7.226-5	4.868-5	3.856-5	3.354-5
2	57	3.531-4	2.883-4	2.469-4	2.202-4	2.020-4	1.893-4	1.657-4	1.654-4	1.713-4	1.792-4
2	58	1.306-3	1.380-3	1.467-3	1.554-3	1.649-3	1.745-3	2.196-3	2.607-3	2.996-3	3.355-3
2	59	5.574-4	4.136-4	3.172-4	2.505-4	2.017-4	1.654-4	7.506-5	4.207-5	2.691-5	1.860-5
2	60	3.765-4	3.027-4	2.549-4	2.232-4	2.013-4	1.856-4	1.532-4	1.484-4	1.513-4	1.569-4
2	61	3.411-4	3.108-4	2.966-4	2.922-4	2.915-4	2.943-4	3.206-4	3.506-4	3.794-4	4.062-4
2	62	1.486-2	1.705-2	1.907-2	2.087-2	2.265-2	2.436-2	3.174-2	3.809-2	4.395-2	4.932-2
2	63	8.151-3	9.355-3	1.047-2	1.148-2	1.244-2	1.338-2	1.743-2	2.092-2	2.413-2	2.708-2
2	64	2.292-6	1.712-6	1.325-6	1.056-6	8.608-7	7.154-7	3.579-7	2.314-7	1.761-7	1.476-7
2	65	1.106-5	1.238-5	1.364-5	1.478-5	1.593-5	1.704-5	2.189-5	2.611-5	3.003-5	3.362-5
2	66	1.114-6	1.065-6	1.052-6	1.060-6	1.073-6	1.094-6	1.209-6	1.322-6	1.429-6	1.527-6
2	67	2.226-6	2.476-6	2.730-6	2.966-6	3.199-6	3.436-6	4.485-6	5.421-6	6.293-6	7.096-6

Table 2. Cont.

I	J	1000	1200	1400	1600	1800	2000	3000	4000	5000	6000
2	68	9.261−7	7.078−7	5.622−7	4.613−7	3.859−7	3.330−7	1.990−7	1.538−7	1.365−7	1.294−7
2	69	7.107−6	8.277−6	9.447−6	1.053−5	1.163−5	1.276−5	1.771−5	2.208−5	2.613−5	2.985−5
2	70	1.898−5	2.196−5	2.475−5	2.733−5	2.976−5	3.221−5	4.267−5	5.174−5	6.011−5	6.778−5
2	71	1.339−7	1.144−7	1.013−7	9.383−8	8.701−8	8.363−8	7.447−8	7.279−8	7.397−8	7.557−8
2	72	1.169−7	9.426−8	7.967−8	6.983−8	6.242−8	5.748−8	4.451−8	3.984−8	3.795−8	3.695−8
2	73	8.133−8	6.208−8	5.020−8	4.219−8	3.648−8	3.270−8	2.279−8	1.919−8	1.751−8	1.658−8
2	74	1.611−7	1.492−7	1.441−7	1.424−7	1.424−7	1.439−7	1.567−7	1.717−7	1.861−7	1.997−7
2	75	2.337−7	1.884−7	1.578−7	1.373−7	1.219−7	1.114−7	8.580−8	7.859−8	7.689−8	7.717−8
2	76	2.474−6	2.688−6	2.894−6	3.090−6	3.266−6	3.435−6	4.119−6	4.662−6	5.128−6	5.539−6
2	77	1.140−6	1.138−6	1.154−6	1.181−6	1.212−6	1.247−6	1.417−6	1.574−6	1.717−6	1.845−6
2	78	6.218−8	3.773−8	2.460−8	1.678−8	1.201−8	8.901−9	2.857−9	1.313−9	0.731−9	0.448−9
2	79	9.433−8	6.978−8	5.481−8	4.511−8	3.794−8	3.337−8	2.132−8	1.690−8	1.484−8	1.369−8
2	80	2.801−7	2.707−7	2.698−7	2.742−7	2.806−7	2.886−7	3.305−7	3.697−7	4.049−7	4.359−7
2	81	4.229−7	3.940−7	3.753−7	3.609−7	3.483−7	3.408−7	3.090−7	2.895−7	2.774−7	2.677−7
2	82	3.821−6	3.942−6	4.033−6	4.156−6	4.196−6	4.292−6	4.543−6	4.742−6	4.967−6	5.151−6
2	83	8.013−7	6.047−7	4.719−7	3.792−7	3.109−7	2.611−7	1.318−7	8.342−8	6.032−8	4.727−8
2	84	2.782−6	3.008−6	3.225−6	3.436−6	3.628−6	3.812−6	4.562−6	5.162−6	5.679−6	6.136−6
2	85	1.469−6	1.516−6	1.570−6	1.609−6	1.646−6	1.683−6	1.786−6	1.848−6	1.900−6	1.945−6
2	86	1.307−4	1.244−4	1.235−4	1.250−4	1.283−4	1.338−4	1.670−4	2.039−4	2.404−4	2.747−4
2	87	1.941−3	1.973−3	2.004−3	2.043−3	2.057−3	2.097−3	2.217−3	2.328−3	2.460−3	2.558−3
2	88	3.779−4	3.787−4	3.810−4	3.857−4	3.877−4	3.937−4	4.152−4	4.366−4	4.610−4	4.803−4
2	89	2.015−4	1.587−4	1.289−4	1.073−4	9.076−5	7.875−5	4.512−5	3.163−5	2.500−5	2.082−5
2	90	3.390−3	3.572−3	3.718−3	3.855−3	3.944−3	4.060−3	4.435−3	4.729−3	5.027−3	5.262−3
2	91	1.792−4	2.024−4	2.277−4	2.532−4	2.783−4	3.054−4	4.283−4	5.394−4	6.429−4	7.394−4
2	92	4.043−4	3.521−4	3.173−4	2.944−4	2.768−4	2.679−4	2.513−4	2.595−4	2.751−4	2.923−4
2	93	8.618−4	1.042−3	1.219−3	1.384−3	1.548−3	1.716−3	2.449−3	3.090−3	3.681−3	4.228−3
2	94	1.811−4	2.077−4	2.365−4	2.652−4	2.935−4	3.237−4	4.603−4	5.829−4	6.968−4	8.030−4
2	95	4.309−3	4.870−3	5.426−3	5.926−3	6.420−3	6.914−3	9.059−3	1.092−2	1.265−2	1.423−2
2	96	7.202−4	5.871−4	5.035−4	4.449−4	4.056−4	3.792−4	3.253−4	3.216−4	3.319−4	3.463−4
2	97	4.919−5	6.610−5	8.345−5	1.005−4	1.171−4	1.344−4	2.121−4	2.809−4	3.442−4	4.032−4
2	98	1.895−4	2.128−4	2.412−4	2.708−4	3.025−4	3.364−4	4.986−4	6.479−4	7.878−4	9.193−4
2	99	1.541−4	1.233−4	1.010−4	8.368−5	7.092−5	6.014−5	3.169−5	1.938−5	1.319−5	9.693−6
2	100	2.797−4	3.622−4	4.487−4	5.330−4	6.183−4	7.067−4	1.109−3	1.466−3	1.796−3	2.103−3
2	101	1.451−4	1.956−4	2.469−4	2.973−4	3.459−4	3.966−4	6.226−4	8.221−4	1.006−3	1.177−3
2	102	8.443−6	6.736−6	5.556−6	4.705−6	4.073−6	3.603−6	2.404−6	1.968−6	1.793−6	1.708−6
2	103	3.389−4	3.252−4	3.200−4	3.201−4	3.233−4	3.286−4	3.647−4	4.024−4	4.376−4	4.704−4
2	104	7.945−4	8.495−4	9.051−4	9.592−4	1.013−3	1.064−3	1.282−3	1.457−3	1.606−3	1.739−3
2	105	4.277−4	4.385−4	4.540−4	4.716−4	4.907−4	5.097−4	5.988−4	6.745−4	7.403−4	7.999−4
2	106	9.861−5	7.657−5	6.100−5	4.977−5	4.116−5	3.480−5	1.754−5	1.058−5	7.066−6	5.100−6
2	107	6.487−4	6.689−4	6.949−4	7.247−4	7.559−4	7.872−4	9.307−4	1.052−3	1.156−3	1.251−3
2	108	4.038−4	3.104−4	2.447−4	1.976−4	1.625−4	1.362−4	6.662−5	3.927−5	2.562−5	1.795−5
2	109	1.216−3	1.387−3	1.540−3	1.679−3	1.806−3	1.923−3	2.394−3	2.751−3	3.047−3	3.309−3
2	110	1.003−3	1.169−3	1.314−3	1.444−3	1.561−3	1.668−3	2.094−3	2.412−3	2.675−3	2.906−3
2	111	3.398−6	3.260−6	3.186−6	3.180−6	3.200−6	3.252−6	3.614−6	4.006−6	4.371−6	4.716−6
2	112	1.288−5	1.426−5	1.570−5	1.702−5	1.836−5	1.966−5	2.552−5	3.066−5	3.540−5	3.978−5
2	113	3.345−6	2.710−6	2.305−6	2.021−6	1.847−6	1.716−6	1.471−6	1.456−6	1.505−6	1.571−6
3	4	2.434−7	2.524−7	2.612−7	2.702−7	2.793−7	2.867−7	3.219−7	3.514−7	3.774−7	4.051−7
3	5	2.748−7	2.877−7	2.988−7	3.079−7	3.175−7	3.250−7	3.555−7	3.787−7	3.991−7	4.208−7
3	6	5.979−7	6.029−7	6.111−7	6.162−7	6.256−7	6.307−7	6.683−7	7.022−7	7.379−7	7.716−7
3	7	3.712−7	4.173−7	4.636−7	5.128−7	5.622−7	6.039−7	8.027−7	9.874−7	1.156−6	1.320−6
3	8	1.561−7	1.329−7	1.172−7	1.065−7	9.907−8	9.407−8	8.289−8	8.127−8	8.264−8	8.504−8
3	9	5.682−7	6.166−7	6.667−7	7.190−7	7.724−7	8.179−7	1.037−6	1.242−6	1.430−6	1.611−6
3	10	1.404−7	1.128−7	9.272−8	7.855−8	6.741−8	5.966−8	3.821−8	3.045−8	2.722−8	2.582−8
3	11	4.125−7	4.922−7	5.692−7	6.469−7	7.223−7	7.902−7	1.094−6	1.369−6	1.618−6	1.854−6
3	12	1.720−7	1.422−7	1.230−7	1.115−7	1.038−7	9.876−8	9.111−8	9.309−8	9.739−8	1.024−7
3	13	2.111−6	2.335−6	2.551−6	2.771−6	2.992−6	3.182−6	4.078−6	4.907−6	5.678−6	6.407−6
3	14	9.870−7	9.036−7	8.339−7	7.916−7	7.484−7	7.196−7	6.251−7	5.842−7	5.771−7	5.669−7
3	15	1.741−7	1.527−7	1.401−7	1.325−7	1.283−7	1.250−7	1.236−7	1.290−7	1.362−7	1.443−7
3	16	2.260−7	2.037−7	1.920−7	1.860−7	1.833−7	1.820−7	1.887−7	2.007−7	2.132−7	2.267−7
3	17	8.645−7	8.777−7	8.892−7	8.962−7	9.083−7	9.120−7	9.469−7	9.793−7	1.020−6	1.053−6
3	18	9.389−8	7.252−8	6.039−8	5.312−8	4.839−8	4.529−8	3.777−8	3.505−8	3.385−8	3.322−8
3	19	9.502−7	9.789−7	1.011−6	1.049−6	1.086−6	1.121−6	1.282−6	1.420−6	1.543−6	1.659−6
3	20	1.223−7	8.849−8	6.767−8	5.399−8	4.458−8	3.761−8	2.072−8	1.423−8	1.112−8	9.255−9

Table 2. Cont.

I	J	1000	1200	1400	1600	1800	2000	3000	4000	5000	6000
3	21	8.107-8	5.416-8	3.995-8	3.193-8	2.714-8	2.418-8	1.916-8	1.879-8	1.935-8	2.016-8
3	22	2.049-6	2.085-6	2.114-6	2.134-6	2.163-6	2.175-6	2.263-6	2.344-6	2.444-6	2.524-6
3	23	6.924-7	6.915-7	6.938-7	7.041-7	7.098-7	7.178-7	7.482-7	7.743-7	8.005-7	8.249-7
3	24	1.476-6	1.460-6	1.442-6	1.420-6	1.403-6	1.385-6	1.294-6	1.225-6	1.181-6	1.150-6
3	25	2.284-6	2.384-6	2.481-6	2.589-6	2.681-6	2.769-6	3.122-6	3.395-6	3.629-6	3.841-6
3	26	2.473-7	2.038-7	1.713-7	1.492-7	1.313-7	1.178-7	8.359-8	7.127-8	6.696-8	6.611-8
3	27	3.614-7	3.642-7	3.662-7	3.699-7	3.733-7	3.763-7	3.937-7	4.110-7	4.309-7	4.484-7
3	28	7.277-7	7.554-7	7.844-7	8.177-7	8.481-7	8.750-7	9.998-7	1.106-6	1.200-6	1.290-6
3	29	9.126-7	9.675-7	1.019-6	1.073-6	1.119-6	1.160-6	1.339-6	1.486-6	1.614-6	1.736-6
3	30	1.284-7	1.111-7	9.847-8	9.081-8	8.573-8	8.250-8	7.992-8	8.656-8	9.566-8	1.053-7
3	31	4.661-7	5.044-7	5.510-7	6.026-7	6.569-7	7.135-7	7.734-7	1.217-6	1.443-6	1.654-6
3	32	4.208-7	3.640-7	3.253-7	3.007-7	2.820-7	2.691-7	2.434-7	2.434-7	2.512-7	2.617-7
3	33	3.590-6	4.181-6	4.759-6	5.320-6	5.866-6	6.419-6	8.815-6	1.098-5	1.297-5	1.481-5
3	34	1.645-4	1.312-4	1.076-4	8.921-5	7.512-5	6.413-5	3.307-5	2.006-5	1.354-5	9.459-6
3	35	4.200-4	5.318-4	6.413-4	7.449-4	8.467-4	9.490-4	1.389-3	1.777-3	2.129-3	2.453-3
3	36	1.813-4	2.313-4	2.803-4	3.264-4	3.719-4	4.176-4	6.138-4	7.866-4	9.431-4	1.088-3
3	37	1.038-4	8.291-5	6.833-5	5.688-5	4.819-5	4.141-5	2.245-5	1.470-5	1.098-5	8.749-6
3	38	4.404-6	3.475-6	2.837-6	2.338-6	1.964-6	1.671-6	8.568-7	5.200-7	3.523-7	2.469-7
3	39	4.390-6	3.764-6	3.386-6	3.129-6	2.975-6	2.897-6	2.947-6	3.318-6	3.771-6	4.228-6
3	40	4.290-5	5.437-5	6.553-5	7.595-5	8.623-5	9.653-5	1.407-4	1.795-4	2.146-4	2.471-4
3	41	3.818-7	2.987-7	2.446-7	2.110-7	1.866-7	1.699-7	1.339-7	1.264-7	1.270-7	1.304-7
3	42	2.367-4	1.909-4	1.586-4	1.362-4	1.175-4	1.041-4	6.736-5	5.312-5	4.705-5	4.456-5
3	43	1.769-5	1.783-5	1.850-5	1.935-5	2.042-5	2.167-5	2.802-5	3.441-5	4.052-5	4.627-5
3	44	5.206-4	5.136-4	5.173-4	5.271-4	5.379-4	5.493-4	6.143-4	6.778-4	7.364-4	7.926-4
3	45	1.524-6	1.206-6	9.942-7	8.341-7	7.155-7	6.254-7	3.865-7	2.974-7	2.591-7	2.390-7
3	46	3.497-6	3.663-6	3.913-6	4.194-6	4.494-6	4.819-6	6.315-6	7.711-6	9.000-6	1.018-5
3	47	1.152-4	9.093-5	7.372-5	6.164-5	5.139-5	4.407-5	2.319-5	1.431-5	9.882-6	7.386-6
3	48	3.454-4	3.391-4	3.402-4	3.457-4	3.516-4	3.587-4	3.991-4	4.396-4	4.773-4	5.131-4
3	49	2.402-7	2.294-7	2.228-7	2.189-7	2.150-7	2.130-7	2.095-7	2.130-7	2.208-7	2.271-7
3	50	1.465-6	1.415-6	1.400-6	1.409-6	1.420-6	1.439-6	1.571-6	1.715-6	1.854-6	1.989-6
3	51	1.246-6	1.124-6	1.055-6	1.017-6	9.906-7	9.772-7	9.866-7	1.042-6	1.109-6	1.178-6
3	52	1.715-7	1.212-7	9.163-8	7.366-8	6.123-8	5.302-8	3.477-8	2.958-8	2.786-8	2.722-8
3	53	4.042-6	3.500-6	3.141-6	2.890-6	2.685-6	2.539-6	2.150-6	2.016-6	1.992-6	1.980-6
3	54	3.064-6	2.996-6	3.002-6	3.046-6	3.099-6	3.159-6	3.503-6	3.845-6	4.163-6	4.466-6
3	55	6.397-6	6.062-6	5.904-6	5.850-6	5.818-6	5.836-6	6.118-6	6.522-6	6.943-6	7.362-6
3	56	1.677-6	1.309-6	1.055-6	8.721-7	7.242-7	6.163-7	3.134-7	1.888-7	1.277-7	9.059-8
3	57	3.782-7	3.484-7	3.322-7	3.252-7	3.207-7	3.198-7	3.342-7	3.596-7	3.864-7	4.133-7
3	58	7.035-7	5.916-7	5.128-7	4.620-7	4.186-7	3.904-7	3.159-7	2.947-7	2.914-7	2.955-7
3	59	1.189-7	7.837-8	5.710-8	4.503-8	3.787-8	3.335-8	2.614-8	2.573-8	2.660-8	2.772-8
3	60	1.692-6	1.702-6	1.744-6	1.809-6	1.876-6	1.941-6	2.270-6	2.567-6	2.829-6	3.074-6
3	61	7.084-7	5.469-7	4.390-7	3.630-7	3.029-7	2.594-7	1.394-7	9.051-8	6.646-8	5.179-8
3	62	1.288-6	1.177-6	1.114-6	1.076-6	1.039-6	1.016-6	9.371-7	8.921-7	8.645-7	8.390-7
3	63	1.975-5	2.037-5	2.096-5	2.152-5	2.190-5	2.234-5	2.392-5	2.530-5	2.678-5	2.789-5
3	64	3.851-4	2.966-4	2.373-4	1.944-4	1.604-4	1.356-4	6.734-5	3.984-5	2.651-5	1.853-5
3	65	2.571-4	2.092-4	1.761-4	1.540-4	1.352-4	1.228-4	8.923-5	7.825-5	7.493-5	7.484-5
3	66	3.377-4	3.246-4	3.217-4	3.248-4	3.294-4	3.359-4	3.768-4	4.193-4	4.589-4	4.963-4
3	67	1.839-3	1.877-3	1.917-3	1.960-3	1.985-3	2.021-3	2.149-3	2.267-3	2.397-3	2.497-3
3	68	2.985-4	2.380-4	1.984-4	1.703-4	1.484-4	1.330-4	9.334-5	8.084-5	7.726-5	7.691-5
3	69	2.428-4	2.296-4	2.243-4	2.240-4	2.247-4	2.279-4	2.502-4	2.760-4	3.007-4	3.244-4
3	70	5.823-3	6.023-3	6.210-3	6.390-3	6.503-3	6.647-3	7.138-3	7.558-3	8.010-3	8.349-3
3	71	3.735-4	3.083-4	2.642-4	2.352-4	2.147-4	2.009-4	1.755-4	1.792-4	1.916-4	2.067-4
3	72	7.785-4	7.271-4	7.038-4	6.977-4	7.020-4	7.151-4	8.167-4	9.392-4	1.063-3	1.182-3
3	73	5.310-4	4.817-4	4.558-4	4.442-4	4.381-4	4.383-4	4.619-4	4.979-4	5.346-4	5.701-4
3	74	3.344-4	2.554-4	2.030-4	1.687-4	1.435-4	1.260-4	8.530-5	7.419-5	7.149-5	7.184-5
3	75	4.088-4	3.649-4	3.391-4	3.252-4	3.183-4	3.171-4	3.411-4	3.840-4	4.309-4	4.771-4
3	76	4.365-4	3.982-4	3.783-4	3.699-4	3.655-4	3.663-4	3.873-4	4.178-4	4.488-4	4.786-4
3	77	3.573-4	3.024-4	2.684-4	2.484-4	2.359-4	2.298-4	2.336-4	2.586-4	2.887-4	3.190-4
3	78	5.931-4	4.371-4	3.343-4	2.626-4	2.105-4	1.723-4	7.719-5	4.305-5	2.744-5	1.888-5
3	79	3.775-4	3.414-4	3.239-4	3.178-4	3.157-4	3.181-4	3.438-4	3.749-4	4.049-4	4.332-4
3	80	3.987-4	2.955-4	2.263-4	1.789-4	1.443-4	1.188-4	5.538-5	3.265-5	2.226-5	1.674-5
3	81	4.215-3	4.751-3	5.267-3	5.740-3	6.196-3	6.654-3	8.619-3	1.034-2	1.192-2	1.337-2
3	82	7.658-3	8.824-3	9.909-3	1.089-2	1.182-2	1.274-2	1.664-2	2.001-2	2.310-2	2.593-2
3	83	4.476-4	3.335-4	2.591-4	2.080-4	1.710-4	1.443-4	7.971-5	5.842-5	4.997-5	4.629-5
3	84	3.289-4	2.794-4	2.500-4	2.333-4	2.223-4	2.166-4	2.133-4	2.246-4	2.388-4	2.534-4
3	85	1.161-2	1.337-2	1.501-2	1.649-2	1.789-2	1.929-2	2.522-2	3.034-2	3.504-2	3.934-2

Table 2. Cont.

I	J	1000	1200	1400	1600	1800	2000	3000	4000	5000	6000
3	86	1.179-6	1.153-6	1.148-6	1.153-6	1.161-6	1.172-6	1.248-6	1.330-6	1.414-6	1.486-6
3	87	1.422-6	1.335-6	1.306-6	1.295-6	1.308-6	1.338-6	1.564-6	1.837-6	2.117-6	2.385-6
3	88	6.263-5	5.783-5	5.616-5	5.564-5	5.632-5	5.798-5	7.052-5	8.560-5	1.008-4	1.153-4
3	89	1.334-4	1.344-4	1.411-4	1.494-4	1.595-4	1.721-4	2.357-4	2.984-4	3.579-4	4.134-4
3	90	6.425-5	5.598-5	5.117-5	4.771-5	4.565-5	4.453-5	4.541-5	5.067-5	5.711-5	6.359-5
3	91	2.842-4	2.672-4	2.583-4	2.503-4	2.452-4	2.422-4	2.379-4	2.422-4	2.520-4	2.593-4
3	92	8.111-6	9.163-6	1.051-5	1.190-5	1.336-5	1.501-5	2.268-5	2.975-5	3.633-5	4.244-5
3	93	2.233-4	1.753-4	1.433-4	1.177-4	9.867-5	8.422-5	4.375-5	2.689-5	1.892-5	1.406-5
3	94	3.735-3	3.871-3	4.013-3	4.108-3	4.199-3	4.285-3	4.618-3	4.890-3	5.183-3	5.392-3
3	95	8.436-6	8.490-6	8.700-6	8.953-6	9.255-6	9.560-6	1.101-5	1.227-5	1.338-5	1.438-5
3	96	6.534-6	6.501-6	6.583-6	6.739-6	6.930-6	7.148-6	8.245-6	9.246-6	1.014-5	1.094-5
3	97	1.642-3	1.676-3	1.715-3	1.744-3	1.776-3	1.805-3	1.935-3	2.048-3	2.168-3	2.261-3
3	98	2.388-4	2.009-4	1.763-4	1.579-4	1.452-4	1.365-4	1.171-4	1.152-4	1.191-4	1.247-4
3	99	3.301-4	3.011-4	2.866-4	2.773-4	2.747-4	2.743-4	2.925-4	3.205-4	3.499-4	3.777-4
3	100	2.342-4	1.931-4	1.657-4	1.451-4	1.306-4	1.202-4	9.493-5	8.893-5	8.952-5	9.220-5
3	101	4.508-4	4.593-4	4.697-4	4.772-4	4.858-4	4.936-4	5.294-4	5.604-4	5.935-4	6.194-4
3	102	1.081-3	1.298-3	1.514-3	1.715-3	1.910-3	2.106-3	2.975-3	3.732-3	4.425-3	5.067-3
3	103	9.161-4	9.849-4	1.064-3	1.141-3	1.219-3	1.302-3	1.678-3	2.017-3	2.332-3	2.623-3
3	104	3.303-4	2.476-4	1.914-4	1.513-4	1.230-4	1.022-4	4.995-5	3.165-5	2.367-5	1.953-5
3	105	4.903-3	5.699-3	6.463-3	7.148-3	7.796-3	8.445-3	1.123-2	1.363-2	1.582-2	1.783-2
3	106	2.294-3	2.640-3	2.972-3	3.265-3	3.547-3	3.822-3	5.010-3	6.031-3	6.964-3	7.820-3
3	107	4.211-4	3.323-4	2.735-4	2.320-4	2.035-4	1.832-4	1.360-4	1.242-4	1.227-4	1.249-4
3	108	3.867-4	3.437-4	3.207-4	3.082-4	3.034-4	3.023-4	3.193-4	3.453-4	3.718-4	3.970-4
3	109	3.579-4	2.890-4	2.446-4	2.142-4	1.943-4	1.805-4	1.528-4	1.504-4	1.547-4	1.612-4
3	110	3.647-4	2.793-4	2.218-4	1.803-4	1.511-4	1.299-4	7.707-5	6.029-5	5.444-5	5.275-5
3	111	3.707-4	4.305-4	5.027-4	5.781-4	6.540-4	7.359-4	1.123-3	1.477-3	1.805-3	2.114-3
3	112	9.909-4	1.046-3	1.105-3	1.167-3	1.227-3	1.286-3	1.544-3	1.753-3	1.930-3	2.091-3
3	113	1.449-3	1.532-3	1.621-3	1.715-3	1.806-3	1.896-3	2.285-3	2.600-3	2.867-3	3.109-3

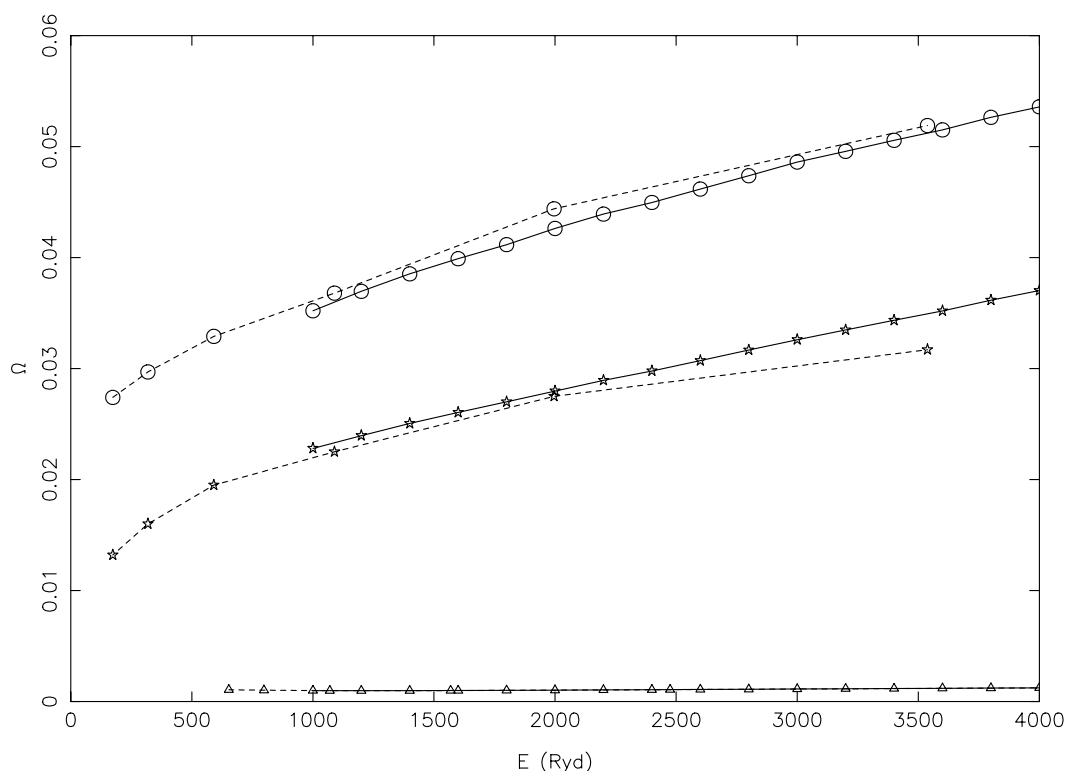
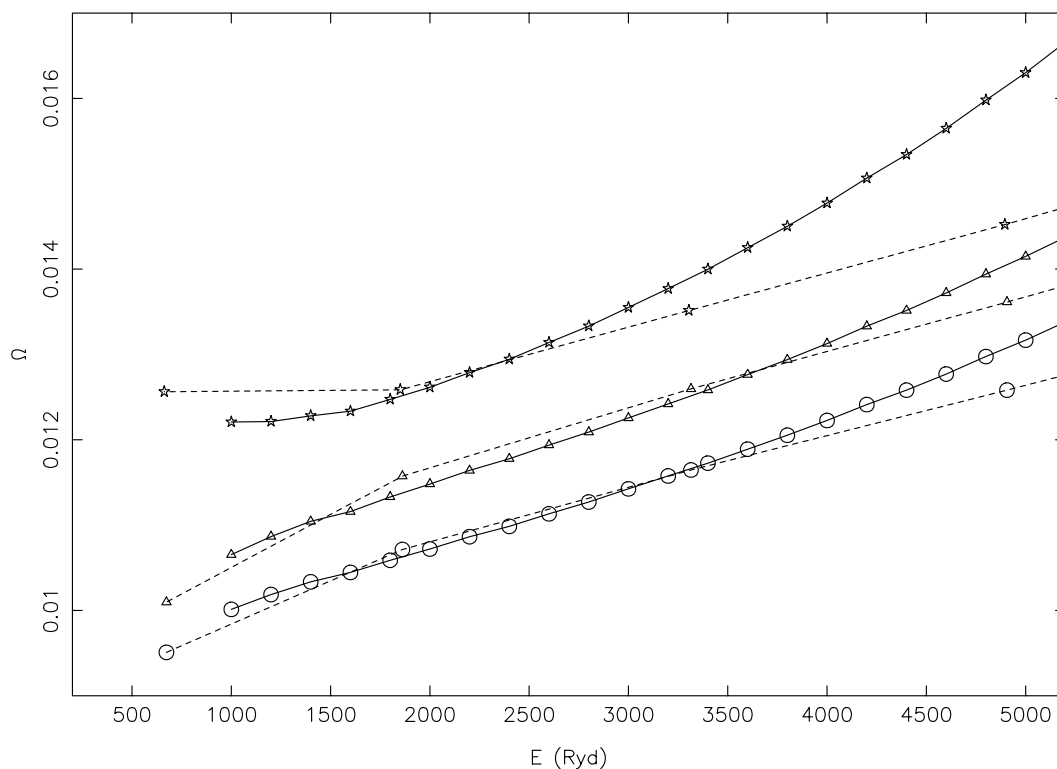


Figure 2. Comparison of collision strengths for the 1–3 ( $2s^2 2p^5 \ ^2P_{3/2}^o - 2s 2p^6 \ ^2S_{1/2}$ ; circles), 1–8 ( $2s^2 2p^5 \ ^2P_{3/2}^o - 2s^2 2p^4 3p \ ^2D_{5/2}^o$ ; triangles), and 2–3 ( $2s^2 2p^5 \ ^2P_{1/2}^o - 2s 2p^6 \ ^2S_{1/2}$ ; stars) transitions of W LXVI. Continuous curves: present results, broken curves: results of Sampson et al. [11].

Finally, in Figure 3, we compare our results of  $\Omega$  from DARC with the corresponding calculations from FAC for three transitions, namely 4–16 ( $2s^22p^43s\ 4P_{5/2}-2s^22p^43d\ 4D_{5/2}$ ), 5–18 ( $2s^22p^43s\ 2P_{3/2}-2s^22p^43d\ 2F_{7/2}$ ), and 8–10 ( $2s^22p^43p\ 2D_{5/2}^o-2s^22p^43p\ 4P_{5/2}^o$ ), all of which are forbidden but have comparatively larger magnitude. Both sets of  $\Omega$  agree well (within 20%), which is highly satisfactory and confirms, once again, that there is no (major) discrepancy among the two present calculations with DARC and FAC, and the earlier one by Sampson et al. [11]. However, we will like to emphasise here the importance of including a large range of partial waves in order to have accurate determination of  $\Omega$ .



**Figure 3.** Comparison of collision strengths for the 4–16 ( $2s^22p^43s\ 4P_{5/2}-2s^22p^43d\ 4D_{5/2}$ : circles), 5–18 ( $2s^22p^43s\ 2P_{3/2}-2s^22p^43d\ 2F_{7/2}$ : triangles), and 8–10 ( $2s^22p^43p\ 2D_{5/2}^o-2s^22p^43p\ 4P_{5/2}^o$ : stars) transitions of W LXVI. Continuous curves: present results from DARC, broken curves: present results from FAC.

In Figure 4, we show the variation of  $\Omega$  for the same three transitions (as shown in Figure 3) with a “top-up” performed at  $J = 30, 40$ , and  $50$ . It is a standard practice to top-up the values of  $\Omega$  with a geometric series for the forbidden transitions. It is clear from this figure that the results topped-up at  $J = 30$  can be overestimated by up to a factor of two, in comparison to those at  $J = 50$ . Similarly,  $\Omega$  obtained with a top-up at  $J = 40$  can be overestimated by up to  $\sim 25\%$ , particularly towards the higher end of the energy range. For this reason, there is scope to slightly further improve the accuracy of  $\Omega$  at high end of the energy range, by further extending the  $J$  range. However, it is not possible due to computational limitations. In conclusion, the accuracy of our calculated  $\Omega$  is comparatively higher (within 20%) for energies up to  $\sim 5000$  Ryd, but may be lower at higher energies. However, it is clearly apparent that the partial waves range ( $\leq 9$ ) included by Goyal et al. [14] is grossly inadequate for the determination of accurate  $\Omega$  values.

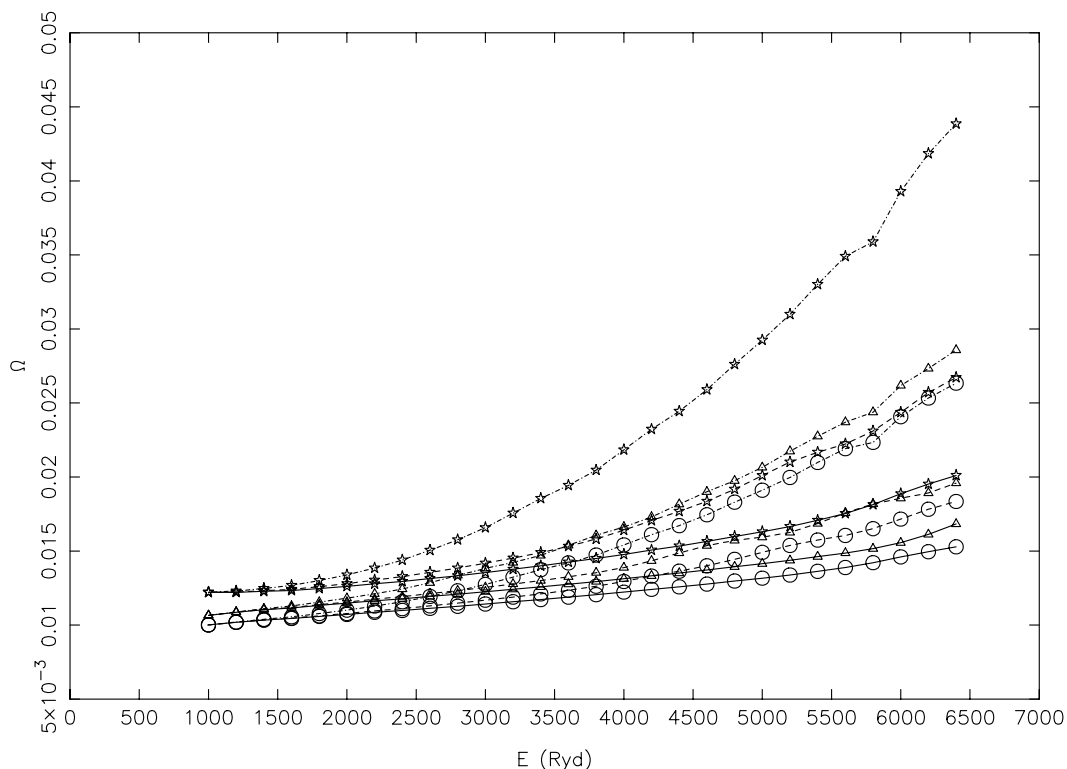


**Figure 4.** Comparison of collision strengths for the 4–16 ( $2s^22p^43s\ 4P_{5/2}-2s^22p^43d\ 4D_{5/2}$ : circles), 5–18 ( $2s^22p^43s\ 2P_{3/2}-2s^22p^43d\ 2F_{7/2}$ : triangles), and 8–10 ( $2s^22p^43p\ 2D_{5/2}^o-2s^22p^43p\ 4P_{5/2}^o$ : stars) transitions of W LXVI. Continuous curves: with top-up at  $J = 50$ , broken curves: at  $J = 40$ , and dotted curves: at  $J = 30$ .

### 3. Conclusions

In this work, we have reported values of  $\Omega$  over a wide range of energy, for transitions among the lowest 113 levels of F-like W LXVI. For the calculations, we have adopted a fully relativistic scattering code DARC, and have included a wide range of partial waves with up to  $J = 50$ , generally sufficient for the convergence of  $\Omega$  for most transitions and at most energies. Nevertheless, to further improve the accuracy of our calculated  $\Omega$ , a top-up has also been included to account for the contribution of higher neglected partial waves. Comparisons of  $\Omega$  have been made with the present and earlier [11] DW calculations and no (major) discrepancy has been noted. Based on these comparisons, the accuracy of our calculated  $\Omega$  is within 20%, for most transitions and at energies up to  $\sim 5000$  Ryd.

A more useful parameter, not considered in the present paper, is *effective* collision strength ( $Y$ ), which is obtained by integrating  $\Omega$  values over a wide energy range and with a suitable electron velocity distribution function, generally Maxwellian. However,  $\Omega$  in the thresholds region does not vary as smoothly as shown in Figures 2 and 3, or in Table 2. Because of the Feshbach (closed channel) resonances, it is a highly varying function of energy, and, therefore, the resonances need to be resolved in a fine energy mesh to accurately determine the values of  $Y$ . With the computational resources presently available to us, such calculations will take several months to conclude, but will be more useful for plasma modelling applications.

**Conflicts of Interest:** The author declares no conflict of interest.

### References

1. Kramida, A.E.; Shirai, T. Energy levels and spectral lines of tungsten, W III through W LXXIV. *At. Data Nucl. Data Tables* **2009**, *95*, 305–474.
2. Kramida, A. Recent progress in spectroscopy of tungsten. *Can. J. Phys.* **2011**, *89*, 551–570.

3. Fournier, K. Atomic data and spectral line intensities for highly ionized tungsten (Co-like  $W^{47+}$  to Rb-like  $W^{37+}$ ) in a high-temperature, low-density plasma. *At. Data Nucl. Data Tables* **1998**, *68*, 1–48.
4. Vilkas, M.J.; López-Encarnación, J.M.; Ishikawa, Y. Relativistic multireference Møller–Plesset perturbation theory calculations of the energy levels and transition probabilities in Ne-like xenon, tungsten, and uranium ions. *At. Data Nucl. Data Tables* **2008**, *94*, 50–70.
5. Safronova, U.I.; Safronova, A.S.; Beiersdorfer, P. Excitation energies, radiative and autoionization rates, dielectronic satellite lines, and dielectronic recombination rates for excited states of Na-like W from Ne-like W. *At. Data Nucl. Data Tables* **2009**, *95*, 751–785.
6. Safronova, U.I.; Safronova, A.S. Wavelengths and transition rates for  $nl-n'l'$  transitions in Be-, B-, Mg-, Al-, Ca-, Zn-, Ag- and Yb-like tungsten ions. *J. Phys. B: At. Mol. Opt. Phys.* **2010**, *43*, 074026.
7. Quinet, P. Dirac-Fock calculations of forbidden transitions within the  $3p^k$  and  $3d^k$  ground configurations of highly charged tungsten ions ( $W^{47+}$ – $W^{61+}$ ). *J. Phys. B: At. Mol. Opt. Phys.* **2011**, *44*, 195007.
8. Aggarwal, K.M.; Keenan, F.P. Energy levels, radiative rates, and lifetimes for transitions in W XL. *At. Data Nucl. Data Tables* **2014**, *100*, 1399–1518.
9. Aggarwal, K.M.; Keenan, F.P. Energy levels, radiative rates, and lifetimes for transitions in W LVIII. *At. Data Nucl. Data Tables* **2014**, *100*, 1603–1767.
10. Aggarwal, K.M.; Keenan, F.P. Radiative rates for E1, E2, M1, and M2 transitions in S-like to F-like tungsten ions (W LIX to W LXVI). *At. Data Nucl. Data Tables* **2016**, *111–112*, 187–279.
11. Sampson, D.H.; Zhang, H.L.; Fontes, C.J. Relativistic distorted-wave collision strengths and oscillator strengths for F-like ions with  $22 \leq Z \leq 92$ . *At. Data Nucl. Data Tables* **1991**, *48*, 25–90.
12. Aggarwal, S. Atomic structure calculations for F-like tungsten. *Chin. Phys. B* **2014**, *23*, 093203.
13. Aggarwal, K.M. Comment on “Atomic structure calculations for F-like tungsten by S. Aggarwal [Chin. Phys B 23 (2014) 093203]”. *Chin. Phys. B* **2016**, *25*, 043201.
14. Goyal, A.; Khatri, I.; Aggarwal, S.; Singh, A.K.; Sharma, R.; Mohan, M. Collisional excitation of fluorine like tungsten using relativistic Dirac atomic R-matrix method. *J. At. Mol. Cond. Nano Phys.* **2015**, *2*, 1–14.
15. Burgess, A.; Sheorey, V.B. Electron impact excitation of the resonance lines of alkali-like positive ions. *J. Phys. B: At. Mol. Opt. Phys.* **1974**, *7*, 2403–2416.



© 2016 by the author; licensee MDPI, Basel, Switzerland. This article is an open access article distributed under the terms and conditions of the Creative Commons Attribution (CC-BY) license (<http://creativecommons.org/licenses/by/4.0/>).